People's Democratic Republic of Algeria
Ministry of Higher Education and Scientific Research
University of Médéa
Faculty of Science



Thesis

Presented to the department of Matter Science
to obtain the degree of

Master of Physics

Discipline: Theoretical physics

By:
Hakim Fourar Laidi

Theme:

Cluster states in bosonic systems : Preparation, entanglement, and quantum computation

05 october 2020

Jury members:

Dr. Abdelhalim Mekhtiche	MCB	University of Medea	President
Dr. Othmane Cherroud	MCB	University of Medea	Examiner
Dr. Karim Bouchachia	MCB	University of Medea	Examiner
Dr. Oussama Houhou	MCB	University of Medea	Supervisor

abstract

We study the generation and entanglement properties of non-Gaussian cluster states of bosonic systems. We consider arbitrary number of harmonic oscillators, and present a protocol to generate, in the long time limit, the target cluster state. Moreover, we show the non-classicality of the obtained states by means of the negativity of the corresponding Wigner function. Also we calculate the amount of entanglement present in the cluster state and discuss a very important use of these states in universal quantum computation.

Keywords: Non-Gaussian states, non-Gaussian cluster states, entanglement, quantum computation, Wigner function negativity.

ملخص

ندرس خصائص التوليد والتشابك للحالات العنقودية غير الغوسية للأنظمة البوزونية. نحن نعتبر عددًا عشوائيًا من المذبذبات التوافقية ، ونقدم بروتوكولًا لإنشاء حالة الكتلة المستهدفة في الحد الزمني الطويل. علاوة على ذلك ، نظهر عدم الكلاسيكية للحالات التي تم الحصول عليها عن طريق سلبية معادلة واگنر المقابلة. نحسب أيضًا مقدار التشابك الموجود في حالة الكتلة ونناقش استخدامًا مهمًا جدًا لهذه الحالات في الحساب الكمي الشامل.

كلمات مفتاحية: الحالات غير الغوسية، الحالات العنقودية غير الغوسية، التشابك، الحساب الكمي، سلبية دالة Wigner .

Author's Declaration

I hereby declare that I am the sole author of this thesis. This is a true copy of the thesis, including any required final revisions, as accepted by my examiners.

إهداء

أهدي مذكرتي هذه إلى التي أوصى بها النبيُّ صلى الله عليه وسلم ثلاثا، إلى مفتاح جنتي و مسكن راحتي، إلى أمي الحبيبة. أخص بالإهاء أيضا إلى من علمني معنى التفاني و الإخلاص، إلى من صبر عليَّ و أواني تحت جناحه، إلى مصنع الرجولة أبتي الغالي.

أهدي مذكرتي هذه أيضا إلى كل العائلة الكريمة كاملة و إلى كل الأصدقاء، عمر و مسلم و يعقوب منهم خاصة.

Acknowledgements

Foremost, I would like to express my sincere gratitude to my advisor Dr. Oussama Houhou for the continuous support of my master graduation, for his patience, motivation, enthusiasm, and immense knowledge. His guidance helped me all the time researching and writing of this thesis. I could not have imagined having a better advisor and supervisor for my study.

I do thank Dr. Abdelhalim Mekhtiche for being the president of the thesis jury. Also I would like to thank Dr. Othmane Cherroud and Dr. Karim Bouchachia for their examination, corrections and insightful comments.

I would like also to thank my family: my parents, brothers and sisters for supporting me through my study time.

Contents

Preface xi

Notation and abbreviations xii

Introduction xiii

1 Quantum systems with continuous variables 1
- 1.1 Quantum harmonic oscillator . . . 1
  - 1.1.1 One-mode QHO . . . 2
  - 1.1.2 Multi-mode QHO . . . 3
- 1.2 Phase-space formalism . . . 4
  - 1.2.1 Quadrature . . . 5
  - 1.2.2 Displacement operator . . . 6
  - 1.2.3 Characteristic function . . . 7
  - 1.2.4 Wigner function . . . 7
  - 1.2.5 First and second moments . . . 8
- 1.3 Gaussian operations and states . . . 8
  - 1.3.1 Gaussian unitaries and symplectic trasformations . . . 9
  - 1.3.2 One-mode Gaussian states and unitaries . . . 10
  - 1.3.3 Multi-modes Gaussian states and unitaries . . . 17
- 1.4 Non-Gaussian operations and states . . . 22
  - 1.4.1 Fock states . . . 23
  - 1.4.2 Schrödinger cat states . . . 23
  - 1.4.3 Cubic phase state . . . 25
- 1.5 Circuit representation of unitaries . . . 26

2 Open quantum systems 28
- 2.1 Open quantum system Dynamics . . . 29

2.1.1 Master equation . . . 29
2.2 Steady state . . . 30
2.2.1 Steady state condition . . . 30
2.3 Examples . . . 30
2.3.1 cooling down oscillators . . . 30
2.3.2 Thermal state . . . 31
2.3.3 One-mode unitary . . . 32
2.3.4 Two-mode unitary . . . 33
2.4 Numerical confirmations of the previous results . . . 36
2.4.1 Fidelity . . . 36
2.4.2 One-mode squeezed vacuum . . . 37
2.4.3 Cubic phase state . . . 37
2.4.4 Two-mode squeezed state . . . 38

3 Non-Gaussian cluster states **39**
3.1 Ideal non-Gaussian cluster states . . . 39
3.1.1 Example: three-mode ideal cluster state . . . 41
3.2 Approximate non-Gaussian cluster states . . . 42
3.3 Switching protocol to generate non-Gaussian cluster states . . . 44
3.3.1 Example of two-modes cluster state . . . 46

4 Entanglement **49**
4.1 Entangled states and partial transposition . . . 50
4.2 Quantifying entanglement . . . 50
4.3 Wigner negativity and mana . . . 51
4.4 Entanglement of formation and Mana for two-mode approximate cluster state . . . 52
4.4.1 Entanglement of formation for two-mode approximate cluster state . . . 52
4.4.2 Wigner function of two-mode cluster state . . . 53
4.4.3 Mana of two-mode cluster state . . . 55

5 Measurement-based quantum computation **57**
5.1 Quantum computation . . . 58
5.2 Universal quantum computaion . . . 59
5.2.1 Continuous-variable quantum gates . . . 59
5.3 Measurement-based quantum computation using continuous variables . . . 60

5.4 Measurement-based computation of two-mode approximate cluster state using Wigner Function 63

Conclusion **65**

A Two-mode squeezing **66**

B The switching programes **68**

C Simulation codes **69**
C.1 Fidelity of examples 69
C.2 Fidelity of two-mode cluster state 71
C.3 Entanglement of formation for tow-mode cluster state 74
C.4 Mana of two-mode cluster state 75

List of Figures

1.1 Wigner function for the vacuum state 11
1.2 Wigner function for a coherent state with $\alpha = 1 + i\frac{3}{2}$. 13
1.3 Wigner function of thermal states at different temperatures. . 14
1.4 Wigner function of squeezed vacuum states, for 3 dB on the top and 6dB on the bootom, in $\hat{p}$ direction on the left ,in $\theta = \pi/4$ in the middele and in $\hat{x}$ direction on the right 16
1.5 A schematic diagram of the beam-splitter(BS), the input states are ρ_{a} and ρ_{b} and the output states are ρ'_{a} and ρ'_{b}. 17
1.6 Wigner function of TMSS, for 3 dB on the top and 6dB on the bootom, in $\hat{p}$ direction on the left, in $\theta = \pi/4$ in the middle and in $\hat{x}$ direction on the right. 20
1.7 Wigner function of two-mode CPHASE state on the right $W^{vac}_{C_Z}$ and on the left $W^{sqez}_{C_Z}$. 23
1.8 Wigner function of Fock states $|0\rangle$, $|1\rangle$, $|2\rangle$, and $|3\rangle$. 24
1.9 Wigner function of cat states: even $|cat_+\rangle$ on the top and odd $|cat_-\rangle$ at the bottom. $\alpha = 1, 5$ on the left and $\alpha = 3$ on the right. 25
1.10 Wigner function of the cubic phase state: on the left $r = 0.5$ and $\tau = 0.2$, on the right $r = 0.3$ and $\tau = 0.8$. 26
1.11 Quantum circuit for: In the top from the left unitary, displacement operator, squeezing operator, till cubic phase gate on the right. At the bottom from the left two mode unitary, controlled phase gate, till beam splitter on the right. 27

2.1 A general representation of OQS interacting with Bath. 28
2.2 Reprentation of OQS losing energies to a bath with rate κ. . . 31
2.3 Reprentation of OQS interacting with a bath while losing energies with rate $\gamma(\bar{n}+1)$ and gaining energies with rate $\gamma\bar{n}$. . . 31

2.4 Reprentation of tow-mode OQS where mode b under unitary acting and mode a losing energies to a bath with rate κ. . . . 32
2.5 Three-mode OQS with mode (a) is loosing energy with rate κ. 34
2.6 Two-mode OQS with mode a loosing energy to a vacuum bath with rate κ. 35
2.7 Fidality Evolution in time for one-mode squeezing in 3dB and 6dB. 37
2.8 Fidality Evolution in time for one-mode cubicity in different $(\tau\ ,\ r)$. 38
2.9 Fidality Evolution in time for one-mode squeezing in different r. 38

3.1 Graphical representation of a N-mode cluster state with arbitrary geometry 40
3.2 Qcircuit representation of an ideal cluster state. 41
3.3 (a) Linear three mode ideal cluster state. (b) Qcircuit representation of Linear three mode ideal cluster state. 42
3.4 Qcircuit representation of circular three mode ideal cluster state. (a) circular three mode ideal cluster state. (b) Qcircuit representation of circular three mode ideal cluster state. 43
3.5 Qcircuit representation of an approximate cluster state. 44
3.6 The physical system proposed to generate the approximate cluster cluster state. 45
3.7 Circuit representation of two-mode approximate cluster state 47
3.8 Fidelity evolution in time for two-mode cluster state with cubicity $\tau = 0.1$ and squeezing 3dB. 48

4.1 Entanglement of formation evolution in squeezing for two-mode cluster state with cubicity $\tau = (0.2, 0.5)$. 53
4.2 Entanglement of formation evolution in τ for two-mode cluster state with squeezing 3dB and 6dB. 54
4.3 Mana evolution in squeezing for two-mode cluster state with cubicity $\tau = (0.2, 0.5)$. 55
4.4 Mana evolution in τ for two-mode cluster state with squeezing 3dB and 6dB. 56

5.1 Circuit representation of a classical computer. 57
5.2 Circuit representation of a quantum computer. 58
5.3 Qcircuit of measuring momentum for entangled state. 62

5.4 Qcircuit of measuring momentum for entangled state with applying unitary on the first mode. 62
5.5 Qcircuit of measuring momentum for tow-mode ideal cluster state. 63
5.6 Qcircuit of measuring momentum for three-mode ideal cluster state. 63
5.7 Qcircuit of measuring momentum for tow-mode ideal cluster state. 64

A.1 A schematic diagram of the beam-splitter(BS), the input states are $|0, r\rangle_{\mathrm{a}}$ and $|0, -r\rangle_{\mathrm{b}}$ and the output state is $|\psi_{s_2}\rangle_{\mathrm{ab}}$. 66

Preface

This study is result of master's thesis in theorical physics in the departement of science of matter, university of Medea, during summer term 2020.

The main contribution of this present work focus on continuous variable quantum systems in order to discuss quantum states, the use of this states to generate non-Gaussian cluster states with the open quantum systems dynamics and its entanglement properties, then we show the role of the resulting cluster states to achieve universal quantum computation.

Notation and abbreviations

CV	Continuous variable
QC	Quantum computation
DV	Discrete variable
QHO	Quantum harmonic oscillator
dB	Decibel
QIP	Quantum information processing
Qubit	Quantum bit
TMSS	Tow-mode squeezed vacuum state
CPHASE	Tow-mode controlled-phase gate
OQS	Open quantum system
GR	Graphical representation
Qcircuit	Quantum circuit
PT	Partiel transpose
$\oplus$	Direct sum
$\otimes$	Tensor product
Tr	Trace
$\|\|.\|\|$	Trace-norm of .
$\|.\|$	Absolut value.
$\mathbb{1}_m$	$m \times m$ identity matrix
$\Re e[z]$	Real part of z
$\Im m[z]$	Imaginary part of z
log	the Natural logarithm
$\log_{10}$	The decimal logarithm

Introduction

Quantum theory is a modern theory, based on Max Planck's quantum hypothesis introduced in 1900. This theory studies the physical properties of systems at the microscopic level.

Computation is data processing, while computers that process input data using the laws of classical physics are called classical computers. The problem with those computer is that they cannot process quantum data. This idea was first supported by Feynman who suggested using quantum systems like simulations of others quantum systems. This lead us through the last two decades to achieve what is called quantum computation.

Quantum computation, also known as quantum information processing, is a processing tool that uses the laws and properties of quantum physics to simulate quantum states. In this case, the information is encoded in states of a simulated quantum system. There are two types of quantum calculations, the first uses the discrete variable which is qubit, and the other uses the continuous variable which is quantum modes. Our study focuses on continuous variables version.

In order to study any system, we can consider it a closed system, i.e., a physical system that does not allow matter and energy to be transferred in or out of the system. But in most realistic situations, the quantum system should be considered as an open system as it interacts with its environment. Our study focuses on open quantum systems.

Universal quantum computation is a very important topic, and we can achieve it using Gaussian cluster states with both Gaussian and non-Gaussian measurements or by non-Gaussian cluster states with Gaussian measurements only. For the remainder of the thesis we focus on the second method.

Continuous variable systems can be bosonic systems which can be photonic or phononic systems, means that our quantum computer can deal with informations using optical, mechanical, electro-optical, electro-mecanical, opto-

mechanical or electro-opto-mechanical systems.

This thesis presents a scheme for the preparation of non-Gaussian cluster states of an open quantum system consisting of arbitrary number of non-interacting harmonic oscillators coupled to a common oscillator that is also damped to the vacuum. The generated cluster state is then used as a resource for universal quantum computation using only Gaussian measurements.

The thesis is organized as the following. In **Chapter 1**, continuous variables systems, phase space formalism, and quantum harmonic oscillator are introduced. Additionally, we present important Gaussian states and their Wigner function in the phase space. Furthermore, we talk about some non-Gaussian states, namely the cubic phase state. In **Chapter 2**, open quantum systems are introduced and their dynamics, in terms of a markovian master equation, are explained. Then we discuss steady states of some examples of open systems. In **Chapter 3**, the definition of non-Gaussian cluster states is given. Also we explain a protocol enabling us to prepare these states in a system of many oscillators. An example of two-mode non-Gaussian cluster state is then studied. **Chapter 4** we discuss entanglement properties of the cluster state, and how to quantify it. In particular, we study the entanglement as function of squeezing and cubicity parameters. **Chapter 5** is devoted to exploiting the cluster state in universal quantum computation. Specifically, we show how one can use the cluster state to implement arbitrary computations in the so called *one-way quantum computation* approach. An example of two-mode cluster is given.

Chapter 1

Quantum systems with continuous variables

Quantum systems can be classified into discret variable (DV) and continuous variable (CV) systems. DV systems have a finite-dimensional Hilbert space, e.g., qudit (**qu**antum **d**-g**it**), a d-dimensional system, where the information is encoded in d-levels state of the system. The most common examples are qubits ($d = 2$) and qutrits ($d = 3$). On the other hand, CV systems have an infinite dimensional Hilbert space. Observables, such as position or momentum, have continuous eigen-spectra, and hence the name *continuous* for this class of quantum systems [1, 2]. CV systems are consisting of N quantised bosonic modes i.e., the quantised harmonique oscillator,which can be described by continuous variables such as position $\hat{X}$ and momentum $\hat{P}$ which are noncommuting Hermitian operators in the Hamiltonian.

1.1 Quantum harmonic oscillator

Quantum harmonic oscillator (QHO) is the quantum mechanical analogue of the classical harmonic oscillator, and it is the foundation for the understanding of complex modes of vibration. our study is about bosonic systems, which can be modelled by a harmonic oscillator.

1.1.1 One-mode QHO

The position and momentum operators for one QHO are given by

$$\hat{X} = \sqrt{\frac{\hbar}{2m\omega}} \left(\hat{a} + \hat{a}^\dagger\right) \ , \tag{1.1}$$

$$\hat{P} = -i\sqrt{\frac{\hbar m\omega}{2}} \left(\hat{a} - \hat{a}^\dagger\right) \ , \tag{1.2}$$

where m is the particle's mass, $\hbar$ is Planck's constant, ω is the (angular) frequency of the oscillator, and $\hat{a}^\dagger$ and $\hat{a}$ are, respectively, the creation and annihilation operators.

In this thesis, we shall use the dimensionless position and momentum, defined as the following:

$$\hat{x} = \sqrt{\frac{m\omega}{\hbar}}\hat{X} \ , \tag{1.3}$$

$$\hat{p} = \sqrt{\frac{1}{\hbar m\omega}}\hat{P} \ , \tag{1.4}$$

and in terms of annihilation and creation operators:

$$\hat{x} = \frac{1}{\sqrt{2}} \left(\hat{a} + \hat{a}^\dagger\right) \ , \tag{1.5}$$

$$\hat{p} = \frac{1}{i\sqrt{2}} \left(\hat{a} - \hat{a}^\dagger\right) \ . \tag{1.6}$$

Usually, we will need to express the creation and annihilaion operators in terms of position and momentum as:

$$\hat{a}^\dagger = \frac{1}{\sqrt{2}} \left(\hat{x} - i\hat{p}\right) \ , \tag{1.7}$$

$$\hat{a} = \frac{1}{\sqrt{2}} \left(\hat{x} + i\hat{p}\right) \ . \tag{1.8}$$

The commutation relation between the position and momentum operators is:

$$[\hat{x}, \hat{p}] = i \ , \tag{1.9}$$

which translates to the following commutation relation for $\hat{a}$ and $\hat{a}^\dagger$:

$$[a, a^\dagger] = 1 \ . \tag{1.10}$$

The Hamiltonian of the one-mode of QHO writes:

$$\hat{H} = \frac{\hbar\omega}{2}(\hat{x}^2 + \hat{p}^2) = \hbar\omega(\hat{a}^\dagger\hat{a} + \frac{1}{2}) \ . \tag{1.11}$$

The action of $\hat{a}$ and $\hat{a}^\dagger$ on an energy eigenstate writes:

$$\hat{a}|n\rangle = \sqrt{n}|n-1\rangle \quad (n \geq 1) \ , \tag{1.12}$$
$$\hat{a}|0\rangle = 0 \ , \tag{1.13}$$
$$\hat{a}^\dagger|n\rangle = \sqrt{n+1}|n+1\rangle \quad (n \geq 0) \ , \tag{1.14}$$

where $|n\rangle$ is the QHO state with n quanta.

The energy eigenstates can be obtained from the vacuum state by iterative application of the creation operator:

$$|n\rangle = \frac{(\hat{a}^\dagger)^n}{\sqrt{n!}}\,|0\rangle \ . \tag{1.15}$$

These states constitute an orthonormal basis,

$$\forall k, n \geq 0, \ \langle n \mid k\rangle = \delta_{k,n} \ , \tag{1.16}$$

and they satisfy the completeness relation

$$\sum_{n=0}^{\infty} |n\rangle\langle n| = \mathbb{1} \ . \tag{1.17}$$

Every state $|\psi\rangle$ can be written in this basis as:

$$|\psi\rangle = \left(\sum_n |n\rangle\langle n|\right)|\psi\rangle \equiv \sum_n c_n\,|n\rangle \ , \tag{1.18}$$

with $c_n = \langle n \mid \psi\rangle$.

1.1.2 Multi-mode QHO

We consider now a set of N QHO. As in the case of one-mode QHO, every QHO is associated the position $\hat{x}_k$, momentum $\hat{p}_k$, and annihilation (creation)

operators $\hat{a}_k$ ($\hat{a}_k^\dagger$), whith $k = 1, \ldots, N$. We write the following:

$$\hat{x}_k = \frac{1}{\sqrt{2}} \left(\hat{a}_k + \hat{a}_k^\dagger \right) , \tag{1.19}$$

$$\hat{p}_k = \frac{1}{i\sqrt{2}} \left(\hat{a}_k - \hat{a}_k^\dagger \right) , \tag{1.20}$$

$$\hat{a}_k = \frac{1}{\sqrt{2}} \left(\hat{x}_k + i\hat{p}_k \right) , \tag{1.21}$$

$$\hat{a}_k^\dagger = \frac{1}{\sqrt{2}} \left(\hat{x}_k - i\hat{p}_k \right) . \tag{1.22}$$

The free Hamiltonian of the system (non interacting modes) is:

$$\hat{H} = \sum_{k=1}^{N} \frac{\hbar\omega_k}{2} (\hat{x}_k^2 + \hat{p}_k^2) = \sum_{k=1}^{N} \hbar\omega_k (\hat{a}_k^\dagger \hat{a}_k + \frac{1}{2}) . \tag{1.23}$$

The action of $\hat{a}_k$ and $\hat{a}_k^\dagger$ on an energy eigenstate is given by:

$$\hat{a}_k |n\rangle_k = \sqrt{n} |n-1\rangle_k \quad (n \geq 1) , \tag{1.24}$$

$$\hat{a}_k |0\rangle_k = 0 , \tag{1.25}$$

$$\hat{a}_k^\dagger |n\rangle_k = \sqrt{n+1} |n+1\rangle_k \quad (n \geq 0) . \tag{1.26}$$

Here, $|n\rangle_k$ is the state of mode k containing n quanta.

The different modes are independent from each other, therefore the commutation relations are written as:

$$[\hat{a}_k, \hat{a}_{k'}^\dagger] = \delta_{kk'} , \tag{1.27}$$

$$[\hat{a}_k, \hat{a}_{k'}] = 0 . \tag{1.28}$$

1.2 Phase-space formalism

The phase space formalism is equivalent to Schrödinger picture of quantum mechanics where instead of using the position or momentum operators we use the eigenvalues of position and momentum, also for the phase space description of quantum states, we use a quasiprobability distribution which is the Wigner function instead of the densite operator in Schrödinger picture.

We shall explicit the notion of quadratures and the use of them in displacement operators using Fourier Weyl relation in order to reach the Wigner function definition formula.

1.2.1 Quadrature

The operators $\hat{x}_k$ and $\hat{p}_k$ are called *quadratures*, and they represent the real and imaginary parts of the annihilation operator $\hat{a}$.

The eigenstates $|x\rangle_x$ and $|p\rangle_p$ of the quadrature operators $\hat{x}$ and $\hat{p}$ are defined as the following:

$$\hat{x}|x\rangle_x = x|x\rangle_x \ , \tag{1.29}$$
$$\hat{p}|p\rangle_p = p|p\rangle_p \ . \tag{1.30}$$

The wave function of the momentum eigenstate is:

$$v_p(x) \equiv_x \langle x \mid p\rangle_p = \frac{1}{\sqrt{2\pi}} e^{ipx}. \tag{1.31}$$

The two eigenstates $|x\rangle_x$ and $|p\rangle_p$ identify two bases which are connected by a Fourier transform

$$|x\rangle_x = \frac{1}{\sqrt{2\pi}} \int dp e^{-ixp} |p\rangle_p, \quad |p\rangle_p = \frac{1}{\sqrt{2\pi}} \int dx e^{ixp} |x\rangle_x. \tag{1.32}$$

These states, $|x\rangle_x$ and $|p\rangle_p$, are *improper* states since they are non-normalizable,

$$\langle x|x'\rangle_x = \delta(x - x') \ , \tag{1.33}$$
$$\langle p|p'\rangle_x = \delta(p - p') \ , \tag{1.34}$$

thus lying outside the Hilbert space. Additionally, we have the following completeness identities:

$$\int_{-\infty}^{\infty} |x\rangle_x \langle x| dx = \mathbb{1} \ , \tag{1.35}$$
$$\int_{-\infty}^{\infty} |p\rangle_p \langle p| dp = \mathbb{1} \ . \tag{1.36}$$

For a multi-mode system, i.e., many QHOs, the commutation relations for the quadratures write:

$$[\hat{x}_k, \hat{p}_{k'}] = i\delta_{kk'} \ , \tag{1.37}$$

where $\hat{x}_k$ and $\hat{p}_k$ are the two quadratures of the k^{th} mode (QHO), $k = 1, \ldots, N$. By arranging the quadratures in a vector, $\hat{Y} = (\hat{x}_1, \hat{p}_1, \ldots, \hat{x}_N, \hat{p}_N)^T$;

T denoting the transpose operation, the commutation relations (1.37)) is simply written

$$[\hat{Y}_k, \hat{Y}_{k'}] = i\Omega_{kk'} \ . \tag{1.38}$$

where $\Omega_{kk'}$ are the elements of the $2N \times 2N$ matrix given by [2, 3]

$$\Omega = \bigoplus_{k=1}^{n} \omega = \begin{pmatrix} \omega & & \\ & \ddots & \\ & & \omega \end{pmatrix} \ , \tag{1.39}$$

with:

$$\omega = \begin{pmatrix} 0 & 1 \\ -1 & 0 \end{pmatrix} \ . \tag{1.40}$$

The Heisenberg uncertainty principle:

$$\Delta x_k \Delta p_k \geq \frac{1}{2} \ . \tag{1.41}$$

1.2.2 Displacement operator

Displacement operators of multi-mode systems are just tensor products of local displacement operators [3]

$$D(\alpha) = \bigotimes_{k=1}^{N} D_k(\alpha_k), \tag{1.42}$$

with $\alpha = (\alpha_1, ..., \alpha_n)^T$, $\alpha_k \in \mathbb{C}$, $k = 1, \ldots, N$ and

$$D_k(\alpha_k) = \exp(\alpha_k a_k^\dagger - \alpha_k^* a_k) \ , \tag{1.43}$$

is the one-mode displacement operator. In term of quadratures, the displacement operator can be written [3]:

$$D(\xi) = \exp(i\hat{Y}^T \Omega \xi) \ , \tag{1.44}$$

with $\xi \in \mathbb{R}^{2N}$ and N number of modes.

1.2.3 Characteristic function

The characteristic function χ of an operator $\hat{\mathcal{O}}$ is [3]

$$\chi[\hat{\mathcal{O}}](\alpha) = \mathrm{Tr}[\hat{\mathcal{O}} D(\alpha)] \,, \tag{1.45}$$

with Tr is the trace, $\alpha \in \mathbb{C}^N$ and $D(\alpha)$ is the displacement operator (1.42).

The characteristic function of a quantum state, described by the density matrix ϱ, is [3]

$$\chi[\varrho](\alpha) = \mathrm{Tr}[\varrho D(\alpha)] \,. \tag{1.46}$$

1.2.4 Wigner function

The Wigner function [4] is a distribution of phase-space associated to a quantum physical system. It partly behaves like a classical probability distribution thus enabling us to calculate measurable quantities such as mean values and variances of the quadratures in a classical way [5]. On the other hand, as opposed to a classical probability distribution, the Wigner function can become negative [6].

The Wigner function of an operator $\hat{\mathcal{O}}$, is defined as the Fourier transform of the characteristic function associated to that operator [3]

$$W[\hat{\mathcal{O}}](\lambda) = \frac{1}{\pi^{2N}} \int_{\mathbb{C}^N} \mathrm{d}^{2N}\lambda \; e^{\alpha^\dagger \lambda + \lambda^\dagger \alpha} \chi[\hat{\mathcal{O}}](\alpha) \,, \tag{1.47}$$

where $\lambda \in \mathbb{C}$. The Wigner function of a state with the density matrix ϱ, $W[\varrho](\lambda)$, is a quasiprobability for the quantum state [3].

We can also write the Wigner function for N-modes in term of the quadrature operators as [2]

$$W(Y) = \int_{\mathbb{R}^{2N}} \frac{d^{2N}\xi}{(2\pi)^{2N}} \exp\left(-iY^T \Omega \xi\right) \chi(\xi) \,, \tag{1.48}$$

where $\xi, Y \in \mathbb{R}^{2N}$ are the eigenvalues of quadratures operators $\hat{Y}$, and $\chi(\xi)$ is the Wigner characteristic function

$$\chi(\xi) = \mathrm{Tr}[\hat{\rho} D(\xi)] \,, \tag{1.49}$$

$D(\xi)$ is the Weyl displacement operator given in **Eq.** (1.44).

1.2.5 First and second moments

The statistical moments of the quantum state are the characteristics of the wigner repesentations (W or χ) [1]. The first moment is called The mean displacement vector (the mean value):

$$\bar{Y} = \langle \hat{Y} \rangle = \mathrm{Tr}(\hat{Y}\hat{\rho}) \, , \tag{1.50}$$

and the second moment is called covariance matrix V:

$$V_{ij} = \frac{1}{2}\langle \{\Delta\hat{Y}_i, \Delta\hat{Y}_j\} \rangle = \frac{1}{2}\mathrm{Tr}(\rho\{\Delta\hat{Y}_i, \Delta\hat{Y}_j\}), \tag{1.51}$$

where $\Delta\hat{Y}_i = \hat{Y}_i - \langle \hat{Y}_i \rangle$ variance of the quadrature $\hat{Y}_i$ and $\{,\}$ anti-commutator. From **Eq.** (1.51) $V_{ij} = V_{ji}$ the covariance matrix is symmetric and from the uncertainty principle **Eq.** (1.41), we can write [2]:

$$V + \frac{i}{2}\Omega \geq 0 \, . \tag{1.52}$$

If we imply the positive definiteness $V > 0$ on **Eq.** (1.38) and from the diagonal terms in **Eq.** (1.52) we can easily get the usual Heisenberg relation for position and momentum [2]

$$V(\hat{x}_k)V(\hat{p}_k) \geq \frac{1}{2} \, . \tag{1.53}$$

1.3 Gaussian operations and states

We may formulate various quantum states relevant to CV quantum information by means of the Wigner representation. The particular quantum states which have only positive Wigner functions (or equivalently the characteristic function χ) that are Gaussian functions are called *Gaussian states*. From the definitions of the Wigner W and characteristic χ functions, one can obtain the following for N-mode systen [2] :

$$\chi(\xi) = e^{\left[-\frac{1}{2}\xi^T(\Omega V \Omega^T)\xi - i(\Omega\bar{Y})^T\xi\right]} \, , \tag{1.54}$$

$$W(Y) = \frac{e^{\left[-\frac{1}{2}(Y-\bar{Y})^T V^{-1}(Y-\bar{Y})\right]}}{(2\pi)^N\sqrt{\det V}} \, . \tag{1.55}$$

Gaussian states are completely characterized by The mean displacement vector $\bar{Y}$ and the covariance matrix V [1]. We write in this case, $\rho = \rho(\bar{Y}, V)$.

The Gaussian operations (or transformations) are those operations that transform the state, but preserve the Gaussian character of any Gaussian input state [2]. In the following we give some Gaussian unitaries that we will use later.

1.3.1 Gaussian unitaries and symplectic trasformations

A unitary U is said to be generated by the Hamiltonian H when the following holds:

$$U = \exp(-itH), \tag{1.56}$$

where t represent time, in the rest of the thesis we take unit time $t = 1$.

A Gaussian unitary U_G is generated by at most a quadratic Hamiltonian H_q of the field operators $\hat{a}_k$ and $\hat{a}_k^\dagger$:

$$H_q = \frac{1}{2}\hat{Y}^T G \hat{Y} + \hat{Y}^T \hat{Y} \ , \tag{1.57}$$

where G is a symmetric matrix, known as the hamiltonian matrix. The Gaussian unitary will be

$$U_G = \exp(-iH_q). \tag{1.58}$$

In the state space, the quantum state ρ of a system transforms as:

$$\rho \longmapsto \rho' = U\rho U^\dagger. \tag{1.59}$$

The most general real linear transformation S which implements the mapping (linear symplectic map) $S : Y \longmapsto Y' = SY'$ must preserve the canonical commutation relations

$$[Y_i', Y_j'] = i\Omega_{ij} \ . \tag{1.60}$$

This is the case exactly if the symplectic matrix S satisfies

$$S\Omega S^T = \Omega. \tag{1.61}$$

The quadratures Y of the field transform in the phase-space, as follows:

$$Y \longmapsto Y' = S.Y + d, \tag{1.62}$$

where $d \in \mathbb{R}^{2N}$ and $S \in \mathbb{R}^{2N\times 2N}$.

Every Gaussian unitary U_G can be decomposed as [2]:

$$U_G = D(d)U_l, \tag{1.63}$$

where $D(d)$ is the Weyl displacement operator (1.44) which corresponds to the symplectic map $Y \longmapsto Y + d$, and the unitary U_l corresponds to the linear symplectic map $S : Y \longmapsto Y' = SY$.

Under the transformation (1.63), the (mean) displacement vector $\langle Y \rangle$ transforms as:

$$\bar{Y} \longmapsto \bar{Y} + d \ , \tag{1.64}$$

and the covariance matrix V transforms as

$$V \longmapsto SVS^T \ . \tag{1.65}$$

1.3.2 One-mode Gaussian states and unitaries

Here we introduce some elementary Gaussian states that play a major role in continuous-variable quantum information.

Vacuum state

The gaussian state with zero quanta in all of the bosonic modes of the field is called *the vacuum state*, and it is denoted $|0\rangle$. The one-mode vacuum state is the zero-eigenstate of the annihilation operator of that mode, **Eq.** (1.25).

The Wigner function for one-mode vacuum state is

$$W_0(Y) = \frac{\exp[-Y^T Y]}{\pi} = \frac{\exp\left[-x^2 - p^2\right]}{\pi} = W_0(x, p). \tag{1.66}$$

In **Figure.** 1.1 we plot the Wigner function of the vacuum. It is clear, from formula and plot, that the vacuum is a Gaussian state.

The mean displacement vector and covariance matrix that are associated to the vacuum stat are:

$$\bar{Y_0} = (0, 0)^T \equiv 0 \ , \tag{1.67}$$

$$V_0 = \frac{1}{2}\mathbb{1}_2. \tag{1.68}$$

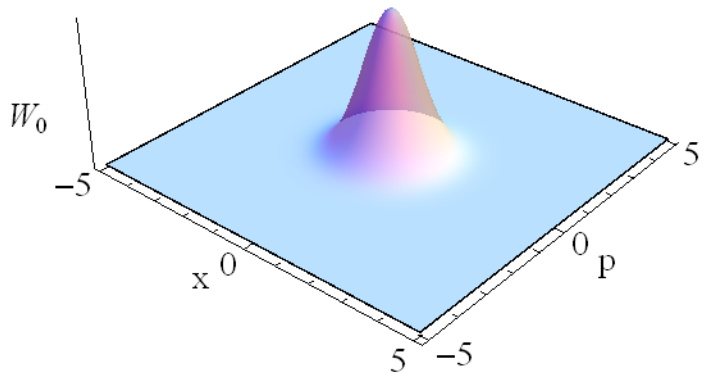


Figure 1.1: Wigner function for the vacuum state

The vacuum state is a state that minimizes the uncertainty principle: the diagonal elements of the covariance matrix (1.68) are the quadratures variances, and therefore it is clear that

$$\Delta x \Delta p = \frac{1}{2}, \tag{1.69}$$

which minimizes the uncertainty principle as said.

coherent state (displaced vacuum)

The displacement operator is generated by the linear Hamiltonian

$$H = i(\alpha \hat{a}^\dagger - \alpha^* \hat{a}) \ , \tag{1.70}$$

and it is defined for one-mode of system by $D(\alpha) = exp(-iH)$ with

$$\alpha = \frac{(\bar{x} + i\bar{p})}{\sqrt{2}} \ , \tag{1.71}$$

where $(\bar{x},\ \bar{p})$ mean values of the position and the momentum respetively.

The coherent state is just a displaced vacuum state

$$|\alpha\rangle = D(\alpha)\,|0\rangle \ . \tag{1.72}$$

It is the eigenstate of the annihilation operator

$$\hat{a}\,|\alpha\rangle = \alpha\,|\alpha\rangle \ . \tag{1.73}$$

Now, we find the displacement and covariance matrix that correspond to the coherent state. The unitary transformation in this case is

$$|0\rangle \longrightarrow |\alpha\rangle = D(\alpha)\,|0\rangle \ . \tag{1.74}$$

Consequently, the annihilation operator transforms by the linear unitary Bogoliubov transformation as

$$\hat{a} \longmapsto \hat{a} + \alpha. \tag{1.75}$$

Then the quadratures $\hat{Y} = (\hat{x}, \hat{p})^T$ follow the transformation

$$\hat{Y} \longmapsto \hat{Y} + d_\alpha, \tag{1.76}$$

where $d_\alpha = \sqrt{2}(\Re[\alpha], \Im[\alpha])^T = (\bar{x}, \bar{p})^T$. The mean displacement vector of the coherent state is $\bar{Y}_c = \bar{Y}_0 + d_\alpha$, but the vacuum state has zero displacement, therefore we write :

$$\bar{Y}_c = d_\alpha \ . \tag{1.77}$$

The covariance matrix of a coherent state with is

$$\begin{aligned} V_c &= \mathbb{1}_2 . V_0 . (\mathbb{1}_2)^T, \\ &= \frac{1}{2}\mathbb{1}_2 \ . \end{aligned} \tag{1.78}$$

From **Eq.** (1.78) it is clear that coherent states minimize also the uncertainty principle given in **Eq.** (1.41).

The Wigner function of the one-mode coherent state can be obtained as

$$\begin{aligned} W_c(x,p) &= \frac{\exp[-(Y-d)^T(Y-d)]}{\pi} \\ &= \frac{\exp[-(x-\bar{x})^2 - (p-\bar{p})^2]}{\pi} \ , \end{aligned} \tag{1.79}$$

and its plot is shown in **Figure.** 1.2.

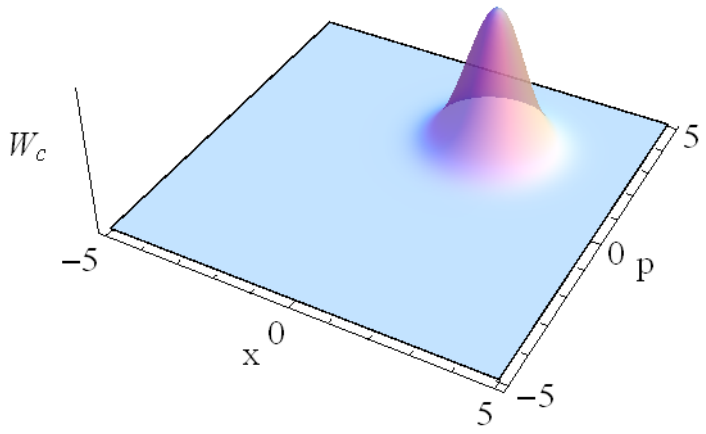


Figure 1.2: Wigner function for a coherent state with $\alpha = 1 + i\frac{3}{2}$.

Thermal states

For a one-mode system at thermal equilibrium with a bath, its state is called *the thermal state*. In the energy eigenstates basis, the density matrix writes [2]

$$\rho_{\text{th}}(\bar{n}) = \sum_{n=0}^{+\infty} \frac{\bar{n}^n}{(\bar{n}+1)^{n+1}} |n\rangle\langle n| \ , \tag{1.80}$$

with $\bar{n}$ is the mean number of quanta present in the bosonic mode,

$$\bar{n} = \langle n|a^\dagger a|n\rangle = (e^{\beta_T} - 1)^{-1} \ , \tag{1.81}$$

where $\beta_T = \hbar\omega/K_B T$, K_B Boltzman constant, and T the temperature which make $\bar{n}$ depend on temperatur $\bar{n} = f(T)$. Notice that when temperature $T \to 0$, the system's state becomes the vacuum.

The mean displacement vector $\bar{Y}_{th}$ and the covariance matrix V_{th} of the one-mode thermal state can be calculated from the definitions, and they read:

$$\bar{Y}_{\text{th}} = (0,0)^T \ , \tag{1.82}$$

$$V_{\text{th}} = \frac{1}{2}\begin{pmatrix} 2\bar{n}+1 & 0 \\ 0 & 2\bar{n}+1 \end{pmatrix} . . \tag{1.83}$$

The Wigner function writes

$$W_{\text{th}}^{\bar{n}}(x,p). = \frac{\exp\left[-\frac{1}{2}Y^T V_{th}^{-1} Y\right]}{\pi(2\bar{n}+1)}, \\ = \frac{\exp(-(x^2+p^2)/(2\bar{n}+1))}{\pi(2\bar{n}+1)} \ , \tag{1.84}$$

and its plot is shown in **Figure.** 1.3.

Notice that the uncertainty principle is depending on $\bar{n}$ where the more we increase the temperature the more the uncertainty principle gets bigger, i.e., $V(\hat{x}_k)V(\hat{p}_k) > \frac{1}{2}$, leading to conclude that the thermal state does not minimize the uncertainty principle given in **Eq.** (1.41).

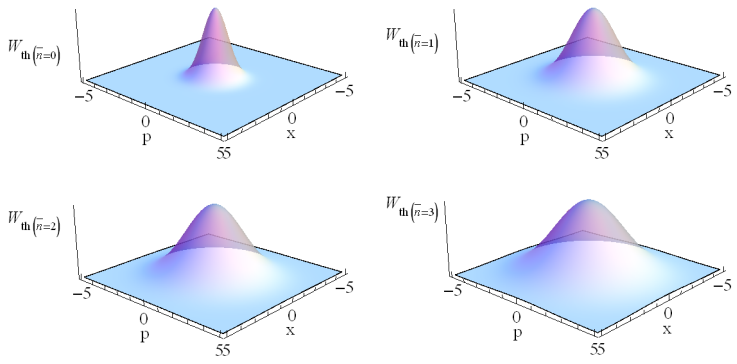


Figure 1.3: Wigner function of thermal states at different temperatures.

Squeezed state

The one-mode squeezing operator is generated by the Hamiltonian

$$H = \frac{i}{2}(\xi^* \hat{a}^2 - \xi(\hat{a}^\dagger)^2) \ . \tag{1.85}$$

Therefore it is defined as:

$$U_s(\xi) = \exp(-iH) = \exp[\frac{1}{2}(\xi^* \hat{a}^2 - \xi(\hat{a}^\dagger)^2)] \ , \tag{1.86}$$

where $\xi = re^{i2\theta}$, $r \geq 0$ the squeezing parameter and $\theta \in [0, \pi]$ the squeezing direction.

The squeezed vacuum state is defined by [2, 6]:

$$|0,\xi\rangle = U_s(\xi)|0\rangle = (1-\tanh|\xi|)^{1/4} e^{\frac{\tanh|\xi|}{2} e^{i\theta}\hat{a}^{\dagger 2}} |0\rangle \ ,$$
$$= (1-\tanh|\xi|)^{1/4} \sum_{n=0}^{\inf} \frac{(\tanh|\xi| e^{i\theta})^n}{2^n n!} \sqrt{(2n)!}\, |2n\rangle \, . \tag{1.87}$$

The first and second moments of the squeezed vacuum state can be easily obtained. The operators $\hat{a}$ and $\hat{a}^\dagger$ transform under the action of the squeezing operator as:

$$\hat{a} \longmapsto (\cosh r)\hat{a} - (e^{i2\theta}\sinh r)\hat{a}^\dagger, \tag{1.88}$$
$$\hat{a}^\dagger \longmapsto (\cosh r)\hat{a}^\dagger - (e^{-i2\theta}\sinh r)\hat{a}. \tag{1.89}$$

Consequently, the quadratures transform like

$$\hat{x} \longmapsto (\cosh r - \sinh r\cos(2\theta))\hat{x} - \sinh r \sin(2\theta)\hat{p} \ , \tag{1.90}$$
$$\hat{p} \longmapsto -\sinh r \sin(2\theta)\hat{x} + (\cosh r + \sinh r\sin(2\theta))\hat{p} \ , \tag{1.91}$$

meaning that the displacement is null and the symplectic map is:

$$S(r,\theta) = \mu \mathbb{1}_2 + R \ , \tag{1.92}$$

with

$$R = \begin{pmatrix} -\Re[\nu] & \Im[\nu] \\ \Im[\nu] & \Re[\nu] \end{pmatrix} \ , \tag{1.93}$$

and $\mu = \cosh r, \nu = e^{-i2\theta}\sinh r$.

Hence, the squeezed vacuum covariance matrix is reads:

$$V_s = \frac{1}{2} S(r,\theta)\mathbb{1}_2 S(r,\theta)^T$$
$$= \begin{pmatrix} \frac{1}{2}(\gamma - \Re[\beta]) & \mu\Im[\nu] \\ \mu\Im[\nu] & \frac{1}{2}(\gamma + \Re[\beta]) \end{pmatrix} \ , \tag{1.94}$$

where $\beta = e^{i2\theta}\sinh(2r)$ and $\gamma = \cosh(2r)$.

The variances (diagonal elements of the covariance matrix) are bellow and above the vacuum noise level [1]. The state described by the covariance matrix (1.94) is said to have a level of squeezing[2] equal to [7]

$$s = 10\log_{10} e^{-2r} \mathrm{dB}.$$

[1] The vacuum noise level is normalized to 1/2, i.e., the vacuum.

[2] The squeezing level is usually quantified in units of decibel (dB)

Interestingly, the squeezed vacuum state minimizes the uncertainty principle, similar to the vacuum and coherent states. This is obvious from **Eq.** (1.94): we have for $\theta = 0$

$$\Delta x \Delta p = \frac{1}{2}\left(\gamma - \Re[\beta]\right)\left(\gamma + \Re[\beta]\right) = \frac{1}{2}\ , \tag{1.95}$$

which as said, is the minimum of the uncertainty principle given in **Eq.** (1.41).

The Wigner function for one-mode squeezed state writes:

$$\begin{aligned} W_s^{r,\theta}(x,p) &= \frac{\exp\left[-\frac{1}{2}Y^T V_s^{-1} Y\right]}{\pi} \\ &= \frac{1}{\pi}\exp\Big[\Re[\nu]\left(p^2 - x^2\right) + 2px\Im[\nu] \\ &\quad - \left(x^2 + p^2\right)\gamma\Big]\ . \end{aligned} \tag{1.96}$$

In **Figure.** 1.4 we plot the Wigner function. It is clear that the shape of the plot is squeezed along a given direction. $\theta = \pi/2$ corresponds to squeezing in $\hat{p}$ direction whereas $\theta = 0$ is for squeezing in $\hat{x}$ direction.

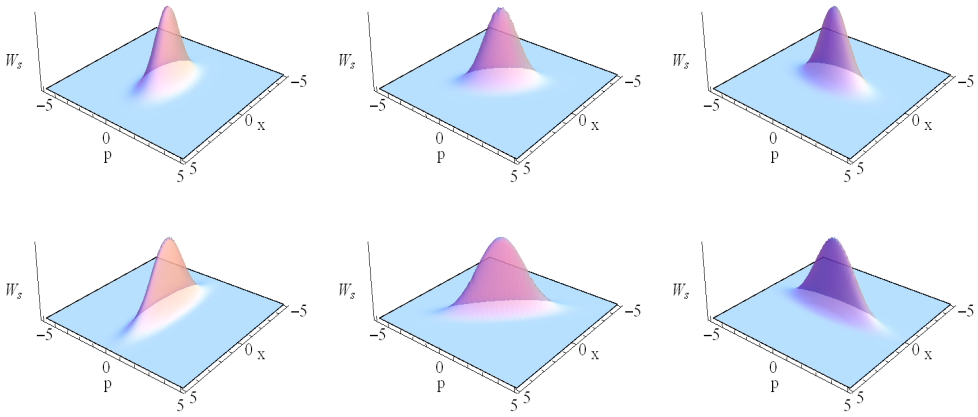


Figure 1.4: Wigner function of squeezed vacuum states, for 3 dB on the top and 6dB on the bootom, in $\hat{p}$ direction on the left ,in $\theta = \pi/4$ in the middele and in $\hat{x}$ direction on the right

1.3.3 Multi-modes Gaussian states and unitaries

Here we introduce some multi-mode Gaussian states that play a major role in quantum information.

Beam splitter

Beam splitters are widely used in the quantum optics and quantum information processing. A beam splitter can work as a type of interferometric device [8]. It accepts two inputs (ρ_a and ρ_b), and produces a two-mode state (ρ'_a and ρ'_b), see **Figure.** A.1.

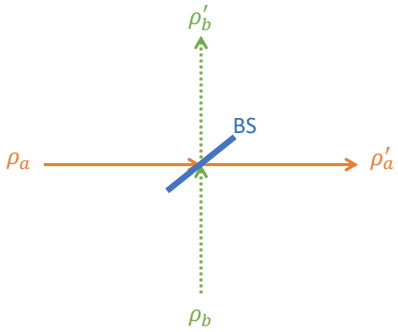


Figure 1.5: A schematic diagram of the beam-splitter(BS), the input states are ρ_{a} and ρ_{b} and the output states are ρ'_{a} and ρ'_{b}.

It is defined with the following unitary:

$$U_{BS}(\zeta) = \exp[\zeta \hat{a}^\dagger \hat{b} - \zeta^* \hat{a} \hat{b}^\dagger)] \ , \tag{1.97}$$

where $\hat{a}$ and $\hat{b}$ are the annihilation operators of the two modes, the coupling strength $\zeta = \phi e^{2i\theta} \in \mathbb{C}$ with $\phi \geq 0$ determines the transmissivity of beam splitter and $\tau = \cos^2 \phi \in [0, 1]$. The beam splitter is called *balanced* when $\tau = 1/2$ and $\theta = 0$.

The symplectic transformation associated to the beam-splitter is obtained in the following. In Heisenberg picture, the annihilation operators undergo the linear Bogoliubov transformation

$$\begin{pmatrix} \hat{a} \\ \hat{b} \end{pmatrix} \mapsto B \begin{pmatrix} \hat{a} \\ \hat{b} \end{pmatrix} \ , \tag{1.98}$$

with

$$B = \begin{pmatrix} \cos\phi & e^{2i\theta}\sin\phi \\ -e^{-2i\theta}\sin\phi & \cos\phi \end{pmatrix} . \tag{1.99}$$

The quadrature operators $\hat{Y} := (\hat{x}_a, \hat{p}_a, \hat{x}_b, \hat{p}_b)^T$ are transformed via the symplectic map

$$\hat{Y} \mapsto S_{BS}\hat{Y} , \tag{1.100}$$

with

$$S_{BS} := \begin{pmatrix} \Re[B] & -\Im[B] \\ \Im[B] & \Re[B] \end{pmatrix} . \tag{1.101}$$

As an example, we consider a balanced beam-splitter, and take the input of it to be diagonal state with covariance matrix of the form

$$V_{input} = \rho_{\rm a} \oplus \rho_{\rm b} = \mathrm{Diag}(\alpha, \beta, \gamma, \sigma) . \tag{1.102}$$

The covariance matrix of the output state of the beam-splitter is

$$V_{BS} = V_{output} = S_{BS} V_{input} S_{BS}^T . \tag{1.103}$$

The explicit formula of the covariance matrix V_{BS} for the balanced beam splitter ($\theta = 0,\ \phi = \pi/4$):

$$\begin{pmatrix} \frac{\alpha+\beta}{2} & \frac{\beta-\alpha}{2} & 0 & 0 \\ \frac{\beta-\alpha}{2} & \frac{\alpha+\beta}{2} & 0 & 0 \\ 0 & 0 & \frac{\gamma+\sigma}{2} & \frac{\sigma-\gamma}{2} \\ 0 & 0 & \frac{\sigma-\gamma}{2} & \frac{\gamma+\sigma}{2} \end{pmatrix} . \tag{1.104}$$

The Wigner Function of the output state, with $\theta = 0$, would take the following simple expression

$$W_{BS}^{\phi,\theta}(x_{\rm a}, p_{\rm a}, x_{\rm b}, p_{\rm b}) = \frac{1}{4\pi^2\sqrt{\alpha\beta\gamma\sigma}} \times e^{-\frac{\sigma\left(\gamma\left(\alpha(p_{\rm a}+x_{\rm a})^2+\beta(p_{\rm a}-x_{\rm a})^2\right)+\alpha\beta(p_{\rm b}-x_{\rm b})^2\right)+\alpha\beta\gamma(p_{\rm b}+x_{\rm b})^2}{4\alpha\beta\gamma\sigma}} . \tag{1.105}$$

Two-mode squeezed state

The two-mode squeezed state (TMSS) is defined by

$$U_{s_2}(\xi)\,|0\rangle \otimes |0\rangle \ , \tag{1.106}$$

where U_{s_2} is the two-mode squeezing operator given by

$$U_{s_2}(\xi) = e^{\xi^* \hat{a}\hat{b} - \xi \hat{a}^\dagger \hat{b}^\dagger} \ , \tag{1.107}$$

with $\hat{a}$ ($\hat{b}$) denotes the annihilation operator of first (second) mode, and $\xi = re^{i2\theta}$, $r \geq 0$ the squeezing parameter and $\theta \in [0, \pi]$ the squeezing direction. The TMSS can be expressed in energy eigenstates basis as [2, 6]

$$|\psi_{s_2}\rangle = U_{s_2} |0\rangle \otimes |0\rangle = \sqrt{1 - \tanh^2 |\xi|} \sum_{n=0}^{\infty} (\tanh |\xi|)^n |n\rangle \otimes |n\rangle \ . \tag{1.108}$$

We should mention that the TMSS can also be obtained by mixing two squeezed vacuum states on a 50:50 beam-splitter, see **Appendix** A for details.

Now, we want to find first and second moments of the TMSS. The field operators $\hat{a}$ and $\hat{a}^\dagger$ transform under the action of U_{s_2} as:

$$\begin{pmatrix} \hat{a} \\ \hat{b}^\dagger \end{pmatrix} \longrightarrow \begin{pmatrix} \mu & -\nu^* \\ -\nu & \mu \end{pmatrix} \begin{pmatrix} \hat{a} \\ \hat{b}^\dagger \end{pmatrix} \ , \tag{1.109}$$

where, as before for single mode squeezing, we have $\mu = \cosh r$ and $\nu = e^{-i2\theta} \sinh r$. Consequently, the quadratures undergo the symplectic map

$$\hat{Y} \to S_{s_2}(r) \hat{Y} \ , \tag{1.110}$$

with

$$S_{s_2}(r) = \begin{pmatrix} \mu \mathbb{1}_2 & R \\ R & \mu \mathbb{1}_2 \end{pmatrix} \ , \tag{1.111}$$

where R is defined in **Eq.** (1.92). From **Eq.** (1.110), it is clear that the TMSS has zero displacement,

$$\bar{Y}_{s_2} = (0, 0, 0, 0) \, , \tag{1.112}$$

and covariance matrix

$$V_{s_2} = \begin{pmatrix} \frac{1}{2}\gamma \mathbb{1}_2 & B \\ B & \frac{1}{2}\gamma \mathbb{1}_2 \end{pmatrix} \ , \tag{1.113}$$

with

$$B = \begin{pmatrix} -\mu \Re[\nu] & \mu \Im[\nu] \\ \mu \Im[\nu] & -\mu \Re[\nu] \end{pmatrix} \ , \tag{1.114}$$

and γ is defined in **Eq.** (1.94). One can easily check that

$$V_{s_2}(\hat{x}_-) = V_{s_2}(\hat{p}_+) = \frac{1}{2}e^{-2\xi}, \tag{1.115}$$

where $\hat{x}_- := (\hat{x}_a - \hat{x}_b)/\sqrt{2}$ and $\hat{p}_+ := (\hat{p}_a + \hat{p}_b)/\sqrt{2}$. Note that for $r = 0$, the TMSS corresponds to two vacuum states and the previous variances are equal to $1/2$, corresponding to the quantum shot-noise. For every two-mode squeezing $r > 0$, we have $V_{s_2}(\hat{x}_-) = V_{s_2}(\hat{p}_+) < 1/2$.

The wigner function for TMSS can be easily calculated,

$$\begin{aligned} W_{s_2}^{r,\theta}(x_1, p_1, x_2, p_2) &= \frac{1}{\pi^2} \exp\left[-\frac{1}{2} Y^T V_{s_2}^{-1} Y\right] \\ &= \frac{1}{\pi^2} \exp\Big[-\big(x_1^2 + x_2^2 + p_1^2 + p_2^2\big)\gamma - 2\big((x_1 x_2 - p_1 p_2)\Re[\nu] \\ &\quad - (x_1 p_2 + x_2 p_1)\Im[\nu]\big)\Big] \ . \end{aligned} \tag{1.116}$$

In **Figure.** 1.6 we plot the Wigner function for fixed $x_2 = 3$ and $p_2 = 2$ and for different squeezing levels and directions.

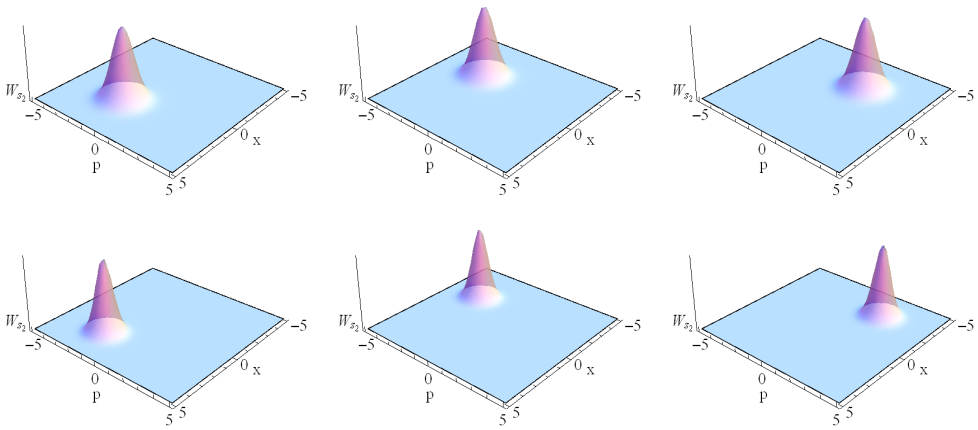


Figure 1.6: Wigner function of TMSS, for 3 dB on the top and 6dB on the bootom, in $\hat{p}$ direction on the left, in $\theta = \pi/4$ in the middle and in $\hat{x}$ direction on the right.

Controlled-phase operation

The controlled-phase operation, denoted *CPHASE* for short, is a multi-mode Gaussian operation defined as

$$U_{C_Z} = \prod_{i,j=1;\ j>i}^{N} U_{C_Z}^{ij} = \prod_{i,j=1;\ j>i}^{N} \exp\left(i g_{ij}(\hat{x}_i \otimes \hat{x}_j)\right) \ , \tag{1.117}$$

which is generated by the Hamiltonian

$$H = -\sum_{i,j=1;\ j>i}^{N} \chi_{ij}(\hat{x}_i \otimes \hat{x}_j), \tag{1.118}$$

where $g_{ij} = \chi_{ij} t$ and χ_{ij} are, respectively, the gain of the interaction and coupling strength between the i^{th} and j^{th} modes, and t denotes the time. The Hamiltonian 1.118 is known as the *quantum non demolition* (QND) coupling [9, 10].

We can mention the resulting of applying all the *CPHASE* operations between the modes according to the adjacency matrix A where its elements are

$$A = [A_{ij}] = [g_{ij}], \tag{1.119}$$

the adjacency matrix has zero elements on the diagonal and this is because the couplings g_{ij} are associated to different modes. and the *CPHASE* operations will be

$$\begin{aligned} U_{C_Z}^{N}(A) &= \prod_{i,j=1;\ j>i}^{N} U_{C_Z}^{ij} = \prod_{i,j=1;\ j>i}^{N} \exp\left(i A_{ij} \hat{x}_i \hat{x}_j\right) \\ &= \exp\left(i \sum_{i,j=1;\ j>i}^{N} A_{ij} \hat{x}_i \hat{x}_j\right). \end{aligned} \tag{1.120}$$

We should mention here that since all the position quadratures mutually commute, then the order in which the *CPHASE* operations are applied is unimportant. Since A is symmetric and has null diagonal elements, then $U_{C_Z}^{N}(A)$ can be written as

$$U_{C_Z}^{N}(A) = \exp\left(\frac{i}{2} \hat{x}^T A \hat{x}\right), \tag{1.121}$$

where $\hat{x} = (\hat{x}_1, \ldots, \hat{x}_N)^T$ the vector of the position quadratures of the N-modes.

The effect of the *CPHASE* gate on the i^{th} and j^{th} modes is given by

$$U_{C_Z}^{ij}|x_i\rangle \otimes |x_j\rangle = \exp\left(i \sum_{i,j=1;\ j>i}^{N} g_{i,j} x_i x_j\right) |x_i\rangle_x \otimes |x_j\rangle_x, \tag{1.122}$$

In the Heisenberg picture, the CPHASE operation transforms the momentum quadratures of the i^{th} and j^{th} modes according to

$$\hat{p}_i \to \hat{p}_i - \sum_{i,j=1;\ j>i}^{N} \hat{x}_j, \tag{1.123}$$

while doing nothing to the position quadratures $\hat{x}_i \to \hat{x}_i$.

If we shoose an arbitrary two-mode diagonal input state $V_{input} = \mathrm{Diag}(a, b, c, d)$ the Wigner function of the controlled phase state will be:

$$W_{C_Z}(x_1, p_1, x_2, p_2) = \frac{\exp\left(\frac{1}{2}\left(-\frac{x_1^2}{a} - \frac{(p_1-x_2)^2}{b} - \frac{x_2^2}{c} - \frac{(p_2-x_1)^2}{d}\right)\right)}{4\pi^2\sqrt{abcd}}. \tag{1.124}$$

If we choose two vacuum states as input states, the wigner function is:

$$W_{C_Z}^{vac}(x_1, p_1, x_2, p_2) = \frac{e^{-p_1^2+2p_1x_2-p_2^2+2p_2x_1-2\left(x_1^2+x_2^2\right)}}{\pi^2}\ . \tag{1.125}$$

And if we choose two squeezed states with $s_1 = -s_2 = 5$ dB and $\theta_1 = \theta_2 = \theta$ as input state, the Wigner function is:

$$\begin{aligned} W_{C_Z}^{sqez}(x_1, p_1, x_2, p_2) \ = \ & \frac{1}{\pi^2}\exp\Big(1.73925\left(-(p_1-x_2)^2 - x_1^2\right) + 1.42302(p_1 \\ & -x_1-x_2)(p_1+x_1-x_2) + 1.42302\left((p_2-x_1)^2 - x_2^2\right) \\ & -1.73925\left((p_2-x_1)^2 + x_2^2\right)\Big) \end{aligned} \tag{1.126}$$

In **Figure.** 1.7 we plot $W_{C_Z}^{vac}$ and $W_{C_Z}^{sqez}$ for $x_2 = p_2 = 0$.

1.4 Non-Gaussian operations and states

When the Wigner function of a state is not Gaussian, we say the the state is *non-Gaussian*. While every quantum state having negative Wigner function is non-Gaussian state, the opposite is not always true, i.e., there exists

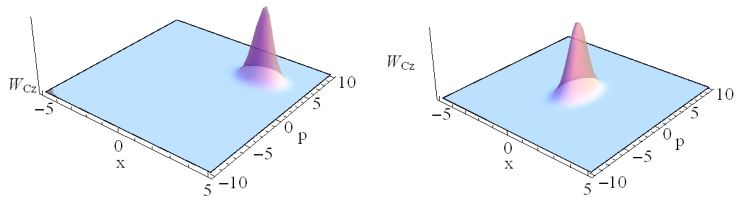


Figure 1.7: Wigner function of two-mode CPHASE state on the right $W_{C_Z}^{vac}$ and on the left $W_{C_Z}^{sqez}$.

some quantum states that have positive Wigner function but they are non-Gaussian. [6]

A Non-Gaussian unitary is a transformation that is generated by at least a cubic order Hamiltonian (polynomial hamiltonian of order 3 in the quadrature operators $\hat{x}$ and $\hat{p}$ of the harmonic oscillator). Obviously, a non-Gaussian unitary will promote Gaussian states to non-Gaussian ones.

1.4.1 Fock states

For a given Fock state (energy eigenstate) $|n\rangle$, the Wigner function is given by [6]:

$$W_{|n\rangle}(x,p) = \frac{(-1)^n}{\pi}\, e^{-\hat{x}^2-\hat{p}^2}\, L_n\left(\frac{\hat{x}^2+\hat{p}^2}{2}\right), \tag{1.127}$$

where L_n denotes the n-th Laguerre polynomial. The vacuum state is included in this formula since $L_0 = 1$. In **Figure.** 1.8 we plot the Wigner function for different Fock states.

1.4.2 Schrödinger cat states

This state was introduced in a thought experiment by Schrödinger [11] in which he highlighted the weird consequences of quantum mechanics when extended to our world (i.e., macroscopic systems). Indeed, superposition of very different states is possible thanks to the superposition principle, for instance the two levels of an atom. How such a situation could happen in our world? In optics, a cat state is a superposition of two coherent states

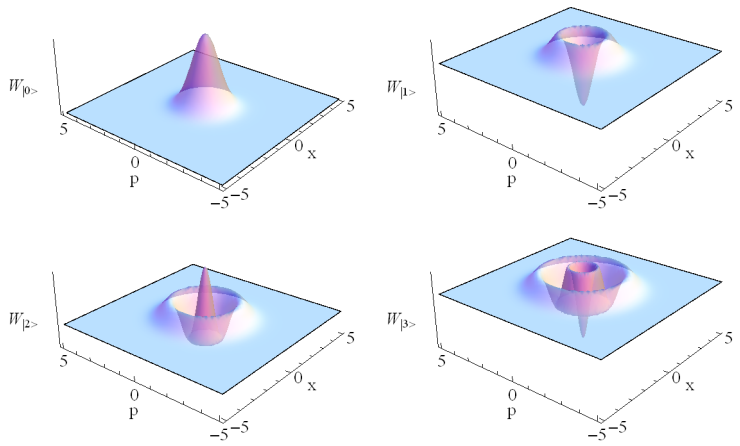


Figure 1.8: Wigner function of Fock states $|0\rangle$, $|1\rangle$, $|2\rangle$, and $|3\rangle$.

[12]

$$|cat_\phi\rangle = \frac{1}{N_\phi}(|\alpha\rangle + e^{i\phi}|-\alpha\rangle) \ , \tag{1.128}$$

where $|\alpha\rangle$ is a coherent state of amplitude α and $N_\phi = \sqrt{2(1+\cos\phi e^{-|\alpha|^2})}$ a normalization factor. The size of the optical cat state is quantified by amplitude α. When α is small we call the state *kitten*.

Two specific cases are interesting. When the phase of the superposition $\phi = 0$, the state is a superposition of even Fock states only and we call this state an *even cat states*:

$$|cat_+\rangle = \frac{1}{N_+}(|\alpha\rangle + |-\alpha\rangle) = \frac{2}{N_+}e^{|\alpha|^2/2}\sum_{n=0}^{+\infty}\frac{\alpha^{2n}}{\sqrt{(2n)!}}|2n\rangle \ . \tag{1.129}$$

With $\phi = \pi$, the state is a superposition of odd Fock states and logically we call it an odd cat state:

$$|cat_-\rangle = \frac{1}{N_-}(|\alpha\rangle - |-\alpha\rangle) = \frac{2}{N_-}e^{|\alpha|^2/2}\sum_{n=0}^{+\infty}\frac{\alpha^{2n+1}}{\sqrt{(2n+1)!}}|2n+1\rangle \ . \tag{1.130}$$

If we choose a quadrature basis such as the amplitude is real ($\alpha \in \mathbb{R}_+$),

the Wigner function of the cat state is [6]

$$\begin{aligned} W_{|cat_\phi\rangle}(x,p) &= \frac{1}{1+\cos\phi e^{-2\alpha^2}}[\frac{1}{2}W_\alpha(x,p)+\frac{1}{2}W_{-\alpha}(x,p) \\ &\quad +\frac{1}{2}W_0(x,\hat{p})\cos(2\alpha\hat{p}/(\sqrt{2})^{-1}-\phi)] \\ &= \frac{e^{-x^2-p^2}}{\pi(1+\cos\phi e^{2\alpha^2})}[e^{\alpha^2}\cosh(2\sqrt{2}\alpha x \\ &\quad +\cos(2\alpha p/(\sqrt{2})^{-1}-\phi] \ . \end{aligned} \tag{1.131}$$

We plot in **Figure.** 1.9 The Wigner function of cat states with different sizes.

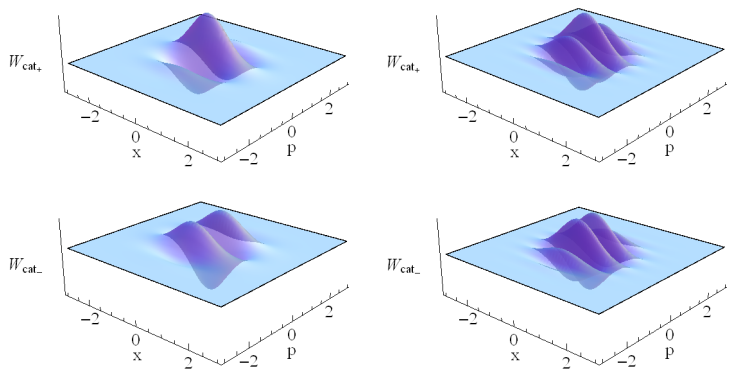


Figure 1.9: Wigner function of cat states: even $|cat_+\rangle$ on the top and odd $|cat_-\rangle$ at the bottom. $\alpha = 1, 5$ on the left and $\alpha = 3$ on the right.

1.4.3 Cubic phase state

The cubic phase gate is defined as [13]

$$U_{C_p}(\tau) = \exp(i\tau\hat{x}^3), \tag{1.132}$$

where $\tau \in \mathbb{R}$ is called the cubicity parameter. Applying this unitary on the zero-momentum eigenstate we obtain the cubic phase state [14],

$$|\tau\rangle = U_{C_p}(\tau)|0\rangle_p = \frac{1}{\sqrt{2\pi}}\int dx e^{i\tau x^3}|x\rangle \ , \tag{1.133}$$

the state $|0\rangle_p$ is obviously unnormalizable (and hence unphysical) state.

By approximating the state $|0\rangle_p$ by highly P-squeezed vacuum, we obtain the so called *approximate cubic phase state*[13, 15],

$$|\tau, r\rangle = U_{C_p}(\tau) U_s(r, \frac{\pi}{2})|0\rangle \ . \tag{1.134}$$

The Wigner function of a cubic phase state is [13]

$$W_{C_p}^{\tau,r}(x,p) = \mathcal{M}_{\tau,r} e^{-\frac{p}{3\tau e^{2r}}} \mathrm{Ai}\left[c\left(3\tau x^2 - p + \frac{1}{12\tau e^{4r}}\right)\right], \tag{1.135}$$

where $c = \left(\frac{4}{3\tau}\right)^{\frac{1}{3}}$, Ai is the Airy function, and $\mathcal{M}_{\tau,r}$ is a normalization coefficient given by

$$\mathcal{M}_{\tau,r} = \frac{e^{\frac{1}{54\tau^2 e^{6r}}}}{\sqrt{\pi} e^r} \left(\frac{4}{3|\tau|}\right)^{\frac{1}{3}} \ . \tag{1.136}$$

In **Figure.** 1.10 we plot the Wigner function of cubic phase state for different cubicity and squeezing parameter.

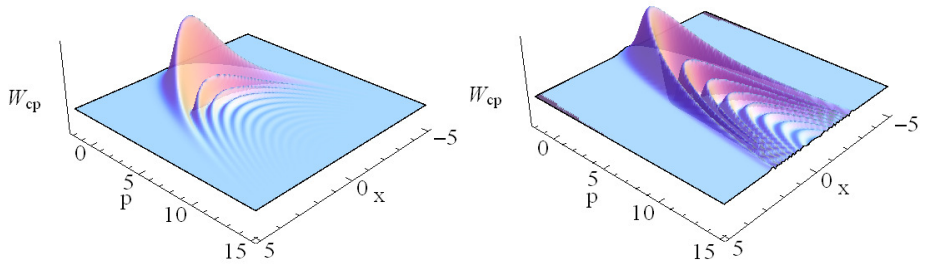


Figure 1.10: Wigner function of the cubic phase state: on the left $r = 0.5$ and $\tau = 0.2$, on the right $r = 0.3$ and $\tau = 0.8$.

1.5 Circuit representation of unitaries

Finally, we note the circuit representation of the quantum unitaries in the quantum circuit (Qcircuit) model of computation in which a computation is a sequence of quantum gates. Some of the studied unitaries are represented in **Figure.** 1.11.

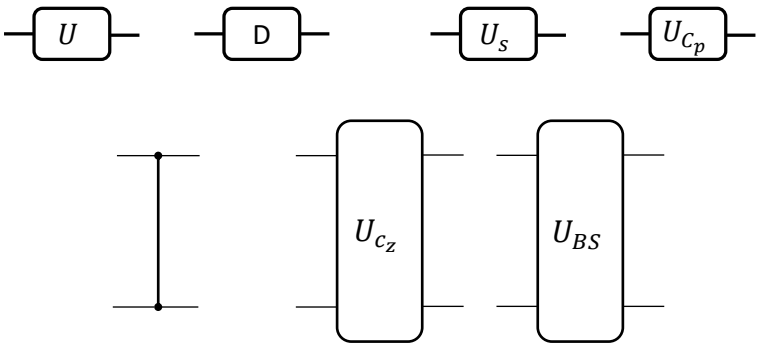


Figure 1.11: Quantum circuit for: In the top from the left unitary, displacement operator, squeezing operator, till cubic phase gate on the right. At the bottom from the left two mode unitary, controlled phase gate, till beam splitter on the right.

Chapter 2

Open quantum systems

In most realistic situations, a quantum system shall be considered as an open quantum system (OQS), coupled to an bath that induces decoherence and dissipation. The dynamics of an OQS can be described, in many cases, with a Markovian master equation. From now on we consider units where $\hbar = 1$.

The composition of a "small" OQS S interacting with a "large" bath B should be considered as a closed system. The OQS S is described by an infinite-dimensional Hilbert space $\mathcal{H}_s = \mathbb{C}^N$,N number of modes and a Hamiltonian H_S, the bath B is described by a very large Hilbert space and a Hamiltonian H_B. The interaction between the OQS and the bath is described by a Hamiltonien H_I, see **Figure.** 2). The total Hamiltonian of the system and bath writes:

$$H_{\text{tot}}(t) = H_s(t) + H_B(t) + H_I(t). \tag{2.1}$$

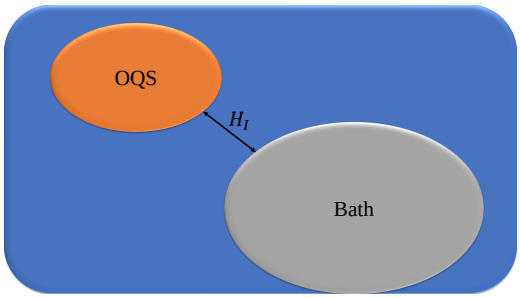


Figure 2.1: A general representation of OQS interacting with Bath.

The total system (OQS + bath) follows unitary dynamics described by Schrödinger equation,

$$\frac{\mathrm{d}\,|\Psi(t)\rangle}{\mathrm{d}t} = -iH_{\mathrm{tot}}(t)\,|\Psi(t)\rangle \ , \tag{2.2}$$

or equivakently in terms of the density matrix $\rho(t)$ of the total system:

$$\frac{\mathrm{d}\rho(t)}{\mathrm{d}t} = i\,[H_{\mathrm{tot}}(t), \rho(t)] \ . \tag{2.3}$$

Since we will be interested in the OQS state, we trace out the bath's degrees of freedom and obtain the reduce density matrix, ρ_s, describing the OQS dynamics:

$$\rho_s(t) = \mathrm{Tr}_B \rho(t) \ . \tag{2.4}$$

2.1 Open quantum system Dynamics

By tracing out the degrees of freedom of the bath in **Eq.** (2.3), we obtain a dynamical equation for the reduced system. We call this latter *master equation* of the OQS.

2.1.1 Master equation

Markovian master equation written in a Liouvillian form is given by [16]

$$\frac{\mathrm{d}\rho_s(t)}{\mathrm{d}t} = -i[H_s(t), \rho_s(t)] + \mathcal{L}[\rho_s(t)] \ , \tag{2.5}$$

where $\mathcal{L}$ is the Liouville superoperator[1], and it has the form

$$\mathcal{L} = \sum_k \left[L_k(t)\rho_s(t)L_k^\dagger(t) - \frac{1}{2}\{L_k^\dagger(t)L_k(t), \rho_s(t)\} \right] \ , \tag{2.6}$$

with $L_k(t)$ are the Liouville operators[2].

[1] A super-operator is a map acting on operators (in this case, the density operator) to give another operator.

[2] They are also called *jump operators*.

2.2 Steady state

In the long time limit the OQS may relax to a steady state,

$$\lim_{t\to\infty} \rho_s(t) = \rho_{ss}, \tag{2.7}$$

that is time-independent density matrix:

$$\lim_{t\to\infty} \frac{\mathrm{d}\rho_s(t)}{\mathrm{d}t} = 0. \tag{2.8}$$

In general, **Eq.** (2.8) my have: (i) one solution that is always independent from initial state of the system, (ii) more than one solution where in this case the steady state will depend on the initial state, or (iii) no solution at all. [15]

2.2.1 Steady state condition

suppose we have, in the long time limit, an arbitrary pure steady state $\rho_{ss} = |\psi\rangle\langle\psi|$. If this is true, then $|\psi\rangle$ must satisfy the following *steady state conditions*:

$$[H_s, \rho_{ss}] = 0 \quad \Rightarrow \quad H_s|\psi\rangle = \varepsilon|\psi\rangle \;\; ; \;\; \varepsilon > 0 \;, \tag{2.9}$$

$$L_k|\psi\rangle = 0 \;. \tag{2.10}$$

2.3 Examples

Here we introduce somme examples of OQSs where we can analytically find their steady states.

2.3.1 cooling down oscillators

We consider a one-mode oscillator (OQS) where its energy is damped to a vacuum bath. Assume that oscillator's Hamiltonian writes $H_s = 0$ and given that there is only one jump operator $L = \sqrt{\kappa}\, a$, where a is the annihilation operator and $\kappa > 0$ denotes the damping rate [17], see **Figure.** 2.3.1.

We want to find the steady states of this system. By applying the steady state conditions we see that first condition is always satisfied while the second one translates to $|\rho_{ss}\rangle = |0\rangle$. This means that the OQS is losing its energy (quanta) and will reach the ground state (vacuum), leading to cooling down the oscillator.

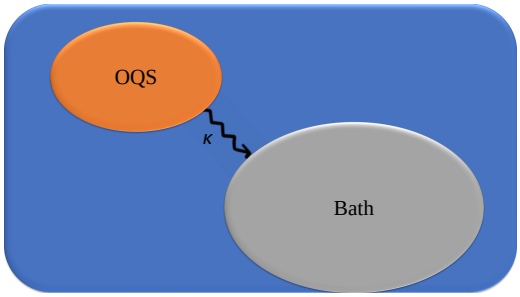


Figure 2.2: Reprentation of OQS losing energies to a bath with rate κ.

2.3.2 Thermal state

Suppose we an oscillator (the OQS), with $H_s = 0$ in a given interaction picture, in a thermal equilibrium with a bath at temperature T. There are two jump operators in this situation: $L_1 = \sqrt{\gamma(\bar{n}+1)}a$ and $L_2 = \sqrt{\gamma\bar{n}}a^\dagger$, see **Figure.** 2.3.2. Here a is the annihilation operator, $\gamma > 0$ denotes the decay rate and $\bar{n}$ is defined in **Eq.** (1.80).

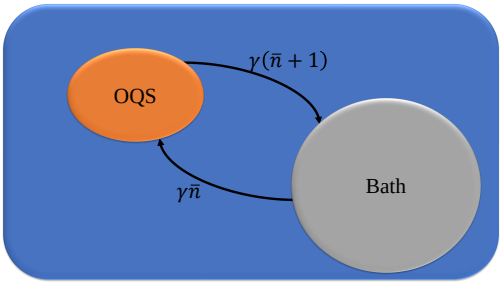


Figure 2.3: Reprentation of OQS interacting with a bath while losing energies with rate $\gamma(\bar{n}+1)$ and gaining energies with rate $\gamma\bar{n}$.

It can be shown that the steady state of this system, called *the thermal state*, has the density matrix [18]

$$\rho_{ss} = \sum_n \frac{(\gamma\bar{n})^n}{(\gamma\bar{n}+1)^{n+1}} |n\rangle\langle n| \ . \tag{2.11}$$

2.3.3 One-mode unitary

Consider two modes interacting with Hamiltonian

$$H_s = g\left(a^\dagger(UbU^\dagger) + a(Ub^\dagger U^\dagger)\right) \ , \tag{2.12}$$

where $g \in \mathbb{R}$ and U unitary acting on mode b only, and assume that one of the two modes, say a, is damped to a vacuum bath: $L = \sqrt{\kappa}a$, see **Figure.** 2.4.

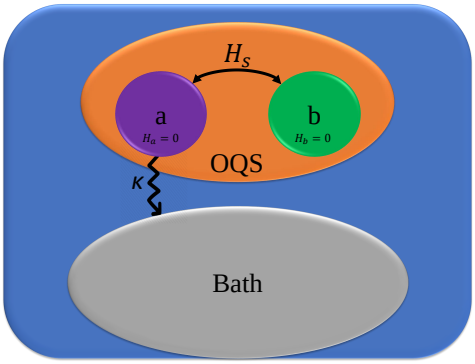


Figure 2.4: Reprentation of tow-mode OQS where mode b under unitary acting and mode a losing energies to a bath with rate κ.

In the following, we find steady state the system may reach. In the long time limit we have:

$$\dot{\rho}_{ss} = -i[H_s, \rho_{ss}] + \kappa\left[a\rho_{ss}a^\dagger - \frac{1}{2}a^\dagger a\rho_{ss} - \frac{1}{2}\rho_{ss}a^\dagger a\right] = 0 \ . \tag{2.13}$$

Put

$$\dot{\rho}'_{ss} = U^\dagger \dot{\rho}_{ss} U \ , \tag{2.14}$$

and

$$H'_s = U^\dagger H_s U = g(a^\dagger b + ab^\dagger) \ . \tag{2.15}$$

Eq. (2.13) changes to

$$\dot{\rho}'_{ss} = -i[H'_s, \rho'_{ss}] + \kappa\left[a\rho'_{ss}a^\dagger - \frac{1}{2}a^\dagger a\rho'_{ss} - \frac{1}{2}\rho'_{ss}a^\dagger a\right] = 0 \ . \tag{2.16}$$

application of the two steady state conditions gives

$$\rho'_{ss} = |00\rangle\langle 00| = U^\dagger \rho_{ss} U \Rightarrow \rho_{ss} = U|00\rangle\langle 00|U^\dagger, \tag{2.17}$$

meaning that the steady state of the system is the pure state $|ss\rangle$:

$$|ss\rangle = |0\rangle \otimes U|0\rangle. \tag{2.18}$$

The nice thing about this approach is that U can be any one-mode unitary. For instance, if $U = U_s(\xi)$ the one-mode squeezing operator defined in **Eq.** (1.87)), the steady state would be vacuum in mode a and the squeezed vacuum in mode b. This can be obtained from a system with the Hamiltonian

$$H_{s_s} = g\left[a\left(\mu b^\dagger + \nu b\right) + a^\dagger\left(\mu b + \nu^* b^\dagger\right)\right], \tag{2.19}$$

where μ and ν are defined in 1.92. The steady state writes

$$|ss\rangle = |0\rangle \otimes U_s(\xi)|0\rangle = |0\rangle \otimes |0, \xi\rangle \ . \tag{2.20}$$

Another example is when $U = U_{Cp}(\tau)U_s(-r)$ where $U_{Cp}(\tau)$ the cubic phase gate and $U_s(-r)$ the squeezing operator with $\theta = \frac{\Pi}{2}$, we would obtain the cubic phase state in mode b:

$$|ss\rangle = |0\rangle \otimes U_{Cp}(\tau)U_s(-r)|0\rangle = |0\rangle \otimes |\tau, r\rangle, \tag{2.21}$$

The Hamiltonian required for the generation of this state is

$$\begin{aligned} H_{s_{Cp}} = g\Big[&\cosh(r)\left(ab^\dagger + a^\dagger b\right) - \sinh(r)\left(ab + a^\dagger b^\dagger\right) \\ &+ \frac{3i\tau}{2\sqrt{2}}\big(\cosh(r) + \sinh(r)\big)\left(a - a^\dagger\right)(b^2 + bb^\dagger + b^\dagger b + b^{\dagger 2})\Big]. \end{aligned} \tag{2.22}$$

2.3.4 Two-mode unitary

Aproach 1

Suppose we have three-mode system with Hamiltonian

$$H_s = g\left(a^\dagger(Ub_1U^\dagger) + a(Ub_1^\dagger U^\dagger)\right) + w\ U\left(b_1^\dagger b_2 + b_1 b_2^\dagger\right)U^\dagger \ , \tag{2.23}$$

where $g, w \in \mathbb{R}$ and U unitary acting on modes b_1 and b_2 only. As Additionally, the mode a is damped to vacuum bath with jump operator $L = \sqrt{\kappa}a$, $\kappa > 0$, see **Figure.** 2.5.

As before, we find the steady state of this system:

$$\dot{\rho}_{ss} = -i[H_s, \rho_{ss}] + \kappa\left[a\rho_{ss}a^\dagger - \frac{1}{2}a^\dagger a\rho_{ss} - \frac{1}{2}\rho_{ss}a^\dagger a\right] = 0. \tag{2.24}$$

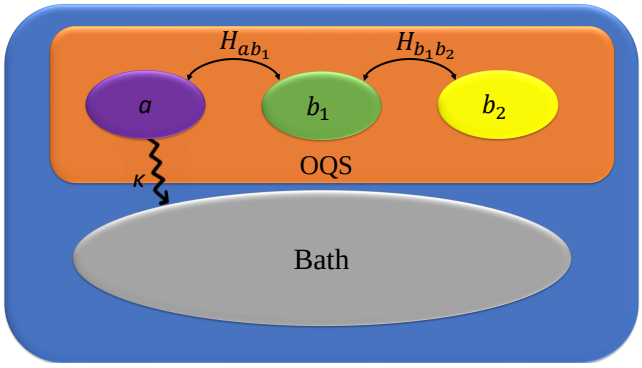


Figure 2.5: Three-mode OQS with mode (a) is loosing energy with rate κ.

Put

$$\dot{\rho}'_{ss} = U^\dagger \dot{\rho}_{ss} U \ , \tag{2.25}$$

and

$$\rho'_{ss} = U^\dagger \rho_{ss} U \qquad H'_s = U^\dagger H_s U = g(a^\dagger b_1 + a b_1^\dagger) + w(b_1^\dagger b_2 + b_1 b_2^\dagger) \ . \tag{2.26}$$

Eq. (2.24) changes to

$$\dot{\rho}'_{ss} = -i[H'_s, \rho'_{ss}] + \kappa \left[a\rho'_{ss}a^\dagger - \frac{1}{2}a^\dagger a \rho'_{ss} - \frac{1}{2}\rho'_{ss}a^\dagger a \right] = 0. \tag{2.27}$$

From the steady state condition we conclude that the system relaxes to the steady state

$$\rho'_{ss} = |000\rangle\langle 000| = U^\dagger \rho_{ss} U \Rightarrow \rho_{ss} = |0\rangle \otimes \left(U |00\rangle \langle 00| U^\dagger \right) \otimes \langle 0| \ , \tag{2.28}$$

i.e., vacuum in mode a and the state $U|00\rangle$ in the other two modes.

Again, U can be any two-mode unitary. For instance, if $U = U_{s_2}(\xi)$ is the two-mode squeezing operator, the steady state of the modes b_1 and b_2 is the two-mode squeezed state. The Hamiltonian giving that state writes

$$\begin{aligned} H_{s_{s_2}} = g\Big[a(\mu b_1^\dagger + \nu b_2) + a^\dagger(\mu b_1 + \nu^* b_2^\dagger)\Big] + w\Big[(\mu^2 + |\nu|^2)(b_1^\dagger b_2 + b_1 b_2^\dagger) \\ + \mu\big(\nu(b_1^2 + b_2^2) + \nu^*(b_1^{\dagger 2} + b_2^{\dagger 2})\big)\Big]. \end{aligned} \tag{2.29}$$

Approach 2

Consider two oscillators with the Hamiltonian

$$H_s = gU\left(a^\dagger b + ab^\dagger\right)U^\dagger, \tag{2.30}$$

where $g \in \mathbb{R}$ and U unitary acting on modes a and b. In addition, let mode a be damped to vacuum bath with $L = \sqrt{\kappa}a$, see **Figure.** 2.31.

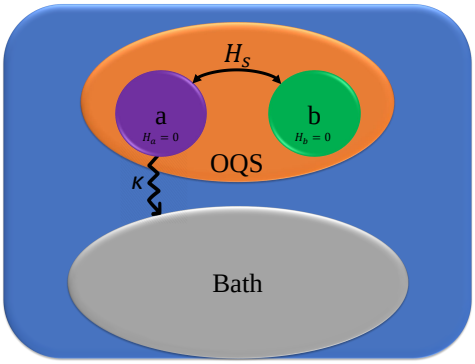


Figure 2.6: Two-mode OQS with mode a loosing energy to a vacuum bath with rate κ.

As before, we find the steady states of the system by starting from the equation

$$\dot{\rho}_{ss} = -i[H_s, \rho_{ss}] + \kappa\left[a\rho_{ss}a^\dagger - \frac{1}{2}a^\dagger a\rho_{ss} - \frac{1}{2}\rho_{ss}a^\dagger a\right] = 0\ , \tag{2.31}$$

and put

$$\dot{\rho}'_{ss} = U^\dagger \dot{\rho}_{ss} U\ , \tag{2.32}$$
$$H'_s = U^\dagger H_s U = g(a^\dagger b + ab^\dagger)\ , \tag{2.33}$$
$$a' = U^\dagger a U\ , \tag{2.34}$$
$$a'^\dagger = U^\dagger a^\dagger U\ . \tag{2.35}$$

The master equation at infinite time becomes

$$\dot{\rho}'_{ss} = -i[H'_s, \rho'_{ss}] + \kappa\left[a'\rho'_{ss}a'^\dagger - \frac{1}{2}a'^\dagger a'\rho'_{ss} - \frac{1}{2}\rho'_{ss}a'^\dagger a'\right] = 0\ . \tag{2.36}$$

The steady state is found from the steady state condition:

$$\rho'_{ss} = |00\rangle\langle 00| = U^\dagger \rho_{ss} U \Rightarrow \rho_{ss} = U|00\rangle\langle 00|U^\dagger \ . \tag{2.37}$$

That is, the steady state of the two modes is

$$|ss\rangle = U|00\rangle. \tag{2.38}$$

Again, the unitary U is arbitrary two-mode operation. e.g., $U = U_{s_2}(\xi)$, two-mode squeezing, the steady state would be

$$|ss\rangle = U_{s_2}|00\rangle = \sqrt{1-\tanh^2|\xi|}\sum_{n=0}^{\infty}(\tanh|\xi|)^n|n\rangle_{b_1}\otimes|n\rangle_{b_2}\ , \tag{2.39}$$

and the corresponding Hamiltonian is

$$\begin{aligned} H_{s_{s_2}} \ &= \ g\Big[(\mu^2+|\nu|^2)(a^\dagger b + a b^\dagger) \\ &\quad +\mu\big(\nu(a^2+b^2)+\nu^*(a^{\dagger 2}+b^{\dagger 2})\big)\Big]. \end{aligned} \tag{2.40}$$

2.4 Numerical confirmations of the previous results

Here we confirm the results of previous sections regarding the steady states. We will be using the fidelity measure in order to demonstrate the dynamics of the system's state and to show that the system indeed reaches the target steady state.

2.4.1 Fidelity

One of the best ways to distinguish two quantum states in quantum computation is the so called fidelity [19]. Fidelity is defined, for two states ρ_1 and ρ_2 as:

$$F(\rho_1,\rho_2) \equiv \left(\mathrm{Tr}\sqrt{\sqrt{\rho_1}\rho_2\sqrt{\rho_1}}\right)^2 \tag{2.41}$$

The fidelity given above is known as *Uhlmann-Jozsa fidelity* [20, 21], and it satisfies the following properties:

1. $0 \leq F(\rho_1, \rho_2) \leq 1$.

2. $F(\rho_1, \rho_2) = 0 \Leftrightarrow \rho_1$ and ρ_2 are orthogonal.

3. $F(\rho_1, \rho_2) = 1 \Leftrightarrow \rho_1$ and ρ_2 are identical.

In what follows, we fix the Hamiltonian of the considered system and solve the corresponding master equation. Then we calculate the fidelity between the the system state at every instant of time and the target steady state. We shall observe the fidelity approaching unit value after a finite evolution time.

2.4.2 One-mode squeezed vacuum

We consider the system with Hamiltonian **Eq.** (2.19) with $g = 10\kappa$. The result of the simulation are shown **Figure.** 2.7. We remark that the more the squeezing the longer evolution time in order for the system to approach the steady state. Consequently, the infinite squeezed state would require infinite time to reach it.

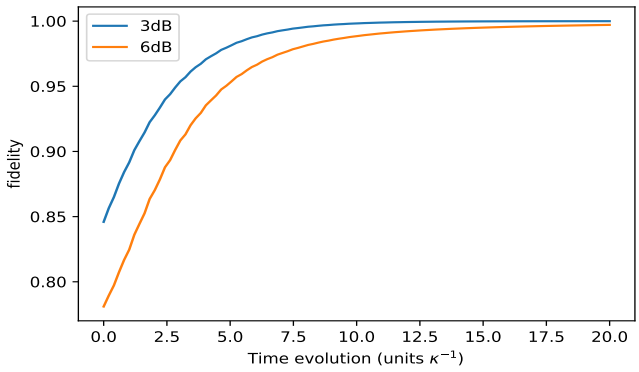


Figure 2.7: Fidality Evolution in time for one-mode squeezing in 3dB and 6dB.

2.4.3 Cubic phase state

With Hamiltonian **Eq.** (2.22) we could produce the plots of **Figure.** 2.4. As in the case of squeezed vacuum above, we see that increasing squeezing or cubicity implies longer times for the system to reach the cubic phase state.

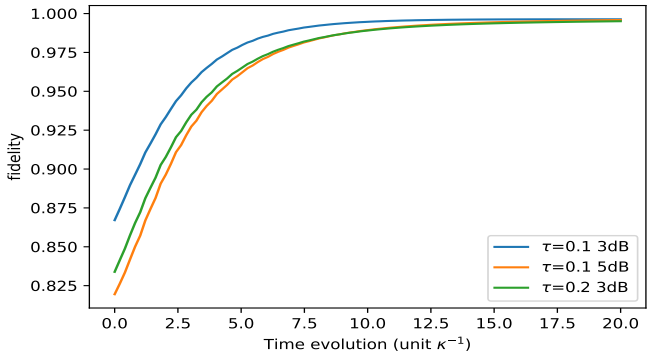


Figure 2.8: Fidality Evolution in time for one-mode cubicity in different $(\tau\ ,\ r)$.

2.4.4 Two-mode squeezed state

With Hamiltonian **Eq.** (2.40) we obtained the plots of **Figure.** 2.9. As expected, high squeezing requies longer times to reach the target two-mode squeezed state.

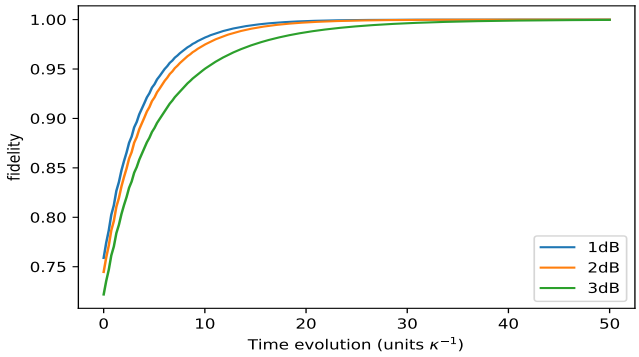


Figure 2.9: Fidality Evolution in time for one-mode squeezing in different r.

Chapter 3

Non-Gaussian cluster states

Cluster states are the resource state for nearly all quantum computer models, and this resource state must be a mutipartite highly entangled state, the first model was introduced by Raussendorf [22] using the DV version of cluster state. The CV was first considered by Lloyd and Braunstein [23] in the circuit model of quantum computing [19]. Years later an equivalent model, the CV version of cluster state was developed by Menicucci and zhang [24, 25]. The CV cluster states are two types, the first one is the the Gaussian cluster states like the one Lloyd and Braunstein provided, and the other type is the non-Gaussian cluster states which have been developed in order to achieve universality without non-Gaussian measurement. In our thesis, we are concerned in the CV non-Gaussian cluster states cases.

3.1 Ideal non-Gaussian cluster states

Cluster states are pure, multi-modes, multi-partite, highly entangled quantum states, and they are important because they allow universal quantum computation given that Gaussian or non-Gaussian [24] measurements are available. If we have a Gaussian cluster state then we need a non-Gaussian measurement and a vis-versa.

Cluster state can be represented by a graphical representation (GR), see **Figure.** 3.1, which has mutually entangled N-mode meaning that it has coupling strength between modes that also leads to a specific geometry (linear, circular, triangular...).

Consider N party system with N-modes, and consider that every mode

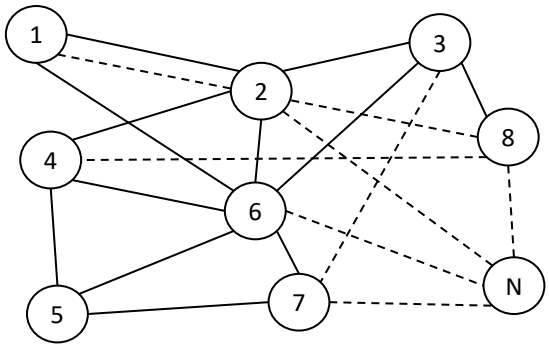


Figure 3.1: Graphical representation of a N-mode cluster state with arbitrary geometry

is in zero momentum eigenstate. If we call this state $|\psi_0\rangle$ then:

$$|\psi_0\rangle = |0\rangle_{p_1} \otimes \cdots \otimes |0\rangle_{p_N}, \tag{3.1}$$

where $|0\rangle_k$ is the zero-momentum eigenstate of the k^{th} mode ($k = 1, \ldots, N$). Since every mode is in a definite zero momentum state, then this means that the momentum variance is zero. According to the uncertainty principle, the variance of the position must be infinite. Therefore, every mode is in an infinite momentum squeezed state which is unphysical state. With applying the cubic phase gate in each mode separately $U^k_{Cp}(\tau_k)$,

$$U_{Cp} = \otimes_{k=1}^{N} U^k_{Cp}(\tau_k) = \otimes_{k=1}^{N} \exp(i\tau_k \hat{x}_k^3), \tag{3.2}$$

we obtain the non-Gaussian cubic phase states in each mode. By creating entanglement between the modes, one obtains the so called *ideal non-Gaussian cluster state* which is unphysical as said before and from now on we call it ideal cluster state. The entangling operation between the i^{th} and j^{th} modes is performed via the application of the *CPHASE* gate defined in **Eq.** (1.117). The constants g_{ij}, with $i, j = 1, \ldots, N$, form a real symmetric matrix, denoted by A, and called *the adjacency matrix* as in Eq.(1.119)

The ideal cluster state $|\psi_I\rangle$ resulting from the quantum circuit (Qcircuit) in **Figure.** 3.2 is therefore written as

$$|\psi_I\rangle = U^N_{CZ}(A) U_{Cp} |\psi_0\rangle, \tag{3.3}$$

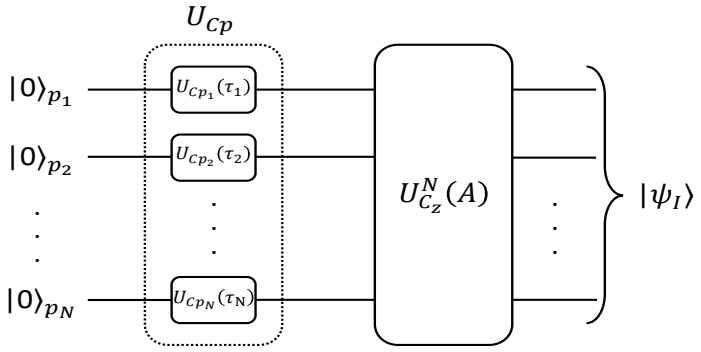


Figure 3.2: Qcircuit representation of an ideal cluster state.

where $U_{C_Z}^N(A)$ is the resultant of applying all the *CPHASE* operations between the modes according to the adjacency matrix A as in Eq.(1.120).

We should mention here that since all the position quadratures mutually commute, then the order in which the *CPHASE* operations are applied is unimportant. Since A is symmetric and has null diagonal elements, then $U_{C_Z}^N(A)$ can be written as

$$U_{C_Z}^N(A) = \exp\left(\frac{i}{2}\hat{x}^T A \hat{x}\right), \tag{3.4}$$

where $\hat{x} = (\hat{x}_1, \ldots, \hat{x}_N)^T$ the vector of the position quadratures of the N-modes.

3.1.1 Example: three-mode ideal cluster state

Suppose we have a linear three mode ideal cluster state, see **Figure.** 3.3. the adjacency in this case

$$A_{\text{lin}} = \begin{pmatrix} 0 & g_{12} & 0 \\ g_{12} & 0 & g_{23} \\ 0 & g_{23} & 0 \end{pmatrix} \tag{3.5}$$

Therefore, $|\psi_I\rangle$ is

$$|\psi_I\rangle = exp\left(i(g_{12}\hat{x}_1\hat{x}_2 + g_{23}\hat{x}_2\hat{x}_3)\right)\left(\otimes_{k=1}^3 \exp(i\tau_k\hat{x}_k^3)\right)|\psi_0\rangle \tag{3.6}$$

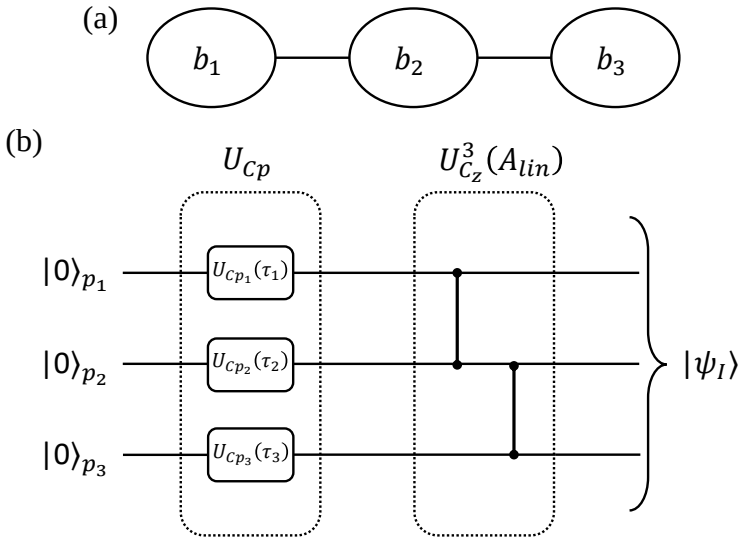


Figure 3.3: (a) Linear three mode ideal cluster state. (b) Qcircuit representation of Linear three mode ideal cluster state.

Now suppose we have a circular three mode ideal cluster state as in **Figure.** 3.4). the adjacency in this case

$$A_{\text{cir}} = \begin{pmatrix} 0 & g_{12} & g_{13} \\ g_{12} & 0 & g_{23} \\ g_{13} & g_{23} & 0 \end{pmatrix} \tag{3.7}$$

and $|\psi_I\rangle$ is

$$|\psi_I\rangle = exp\left(i(g_{12}\hat{x}_1\hat{x}_2 + g_{23}\hat{x}_2\hat{x}_3 + g_{13}\hat{x}_1\hat{x}_3)\right)\left(\otimes_{k=1}^{3}\exp(i\tau_k\hat{x}_k^3)\right)|\psi_0\rangle \tag{3.8}$$

3.2 Approximate non-Gaussian cluster states

In order to generate a physical non-Gaussian cluster state $|\psi_P\rangle$ we need to approximate the zero momentum state with highly squeezed state in the p-direction. we have the following limit.

$$|0\rangle_p = \lim_{r\to\infty} U_s(-r)|0\rangle \qquad \Rightarrow \qquad \lim_{r\to\infty}|\psi_P(r)\rangle = |\psi_I\rangle. \tag{3.9}$$

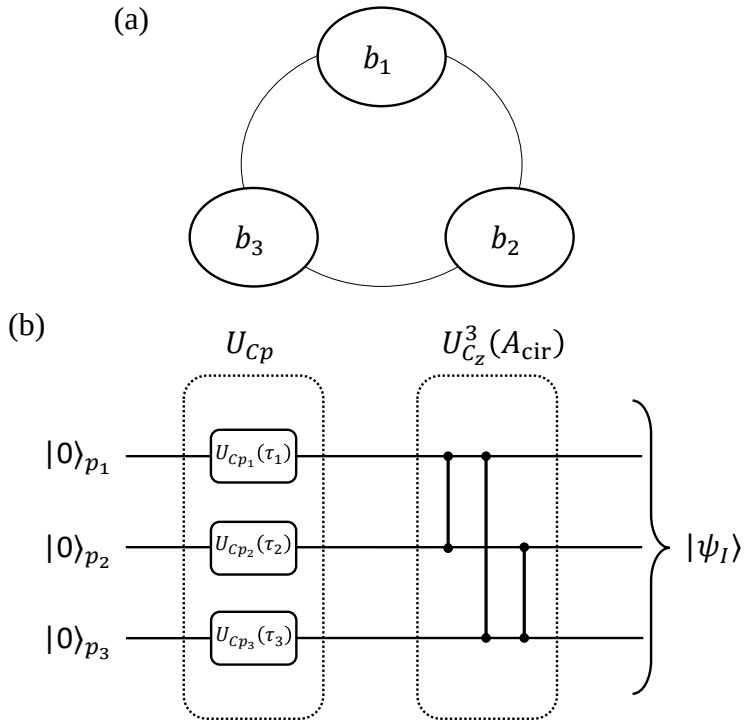


Figure 3.4: Qcircuit representation of circular three mode ideal cluster state. (a) circular three mode ideal cluster state. (b) Qcircuit representation of circular three mode ideal cluster state.

therfore, the approximate cluster state in this case is

$$|\psi_P\rangle = U_{C_Z}^N(A) U_{Cp} U_s |0\rangle^N , \tag{3.10}$$

where $|0\rangle^N = |0\rangle_1 \otimes \cdots \otimes |0\rangle_N$ and

$$U_s = \otimes_{k=1}^N U_{s_k}(-r_k) \qquad \Leftrightarrow \qquad U_{s_k}(-r_k) = \exp\left(-\frac{r_k}{2}(a_k^2 - a_k^{\dagger 2})\right). \tag{3.11}$$

to obtain an approximated $|\psi_P\rangle$, $r \equiv$ should be finite value. In **Figure.** 3.5 we give Qcircuit of the approximate cluster state.

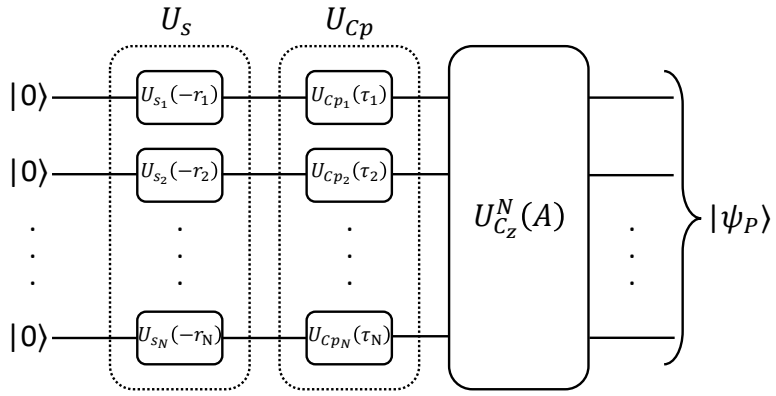


Figure 3.5: Qcircuit representation of an approximate cluster state.

3.3 Switching protocol to generate non-Gaussian cluster states

In this section we present the approach to generate $|\psi_P\rangle$ as the steady state of N-mode system coupled to a common mode a in the OQS [13, 26], see **Figure.** 3.6.

The reason why we choose this approach is that the physicist always look for the easiest way to get results, and this is an easy way to get the target results, also even easy experimentally where it is easier to study a group system of independent harmonic oscillators then to study a group system of interacting harmonic oscillators.

Our protocol in order to generate $|\psi_P\rangle$ is switching scheme [13]. Swiching scheme is about considering an OQS consisting of N-mode system coupled to a common mode a of **Figure.** 3.6. The proposed Hamiltonian of this system is [13]

$$H = a^\dagger \sum_k \left(g_1^{(k)} b_k + g_2^{(k)} b_k^\dagger + g_3^{(k)} b_k^2 + g_4^{(k)} {b_k^\dagger}^2 + g_5^{(k)} \{b_k, b_k^\dagger\} \right) + \text{H.c.} \,, \quad (3.12)$$

where H.c hermetian conjugate of the first part of H and a (b_k) is the common mode (k^{th} mode) annihilation operator, and $g_\mu^{(k)}$ ($\mu = 1, \ldots, 5$) are the couplings strength. the dynamics of the OQS is described by a master equation

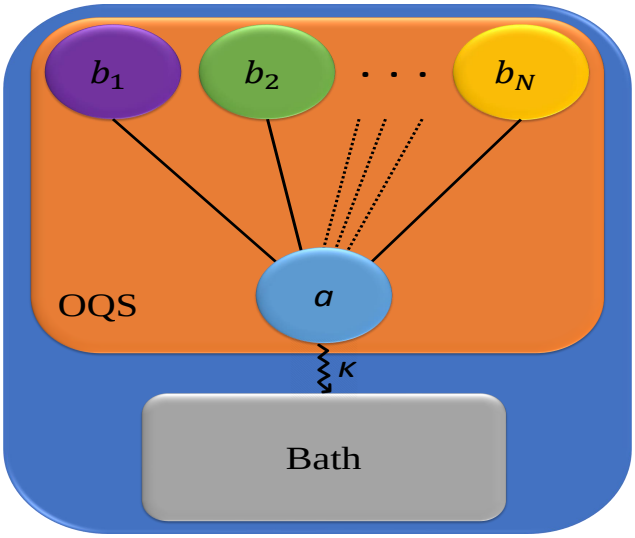


Figure 3.6: The physical system proposed to generate the approximate cluster cluster state.

given by [27, 17]

$$\frac{\mathrm{d}\rho(t)}{\mathrm{d}t} = -i[H, \rho(t)] + \kappa a \left(\rho a^\dagger - \frac{1}{2} \left\{ a^\dagger a, \rho \right\} \right) \ , \tag{3.13}$$

where ρ is the OQS's density operator, κ damping rate of the common mode.

Our goal is to find the steady state of the modes at the last step which will give as the non-Gaussian cluster state. Our protocol is composite of N consecutive steps, where in each step we perform the following transformation:

$$b_\ell \longrightarrow d_\ell = \left[U_{C_Z}^N(A) U_{Cp} U_s \right] \ b_\ell \ \left[U_{C_Z}^N(A) U_{Cp} U_s \right]^\dagger \qquad (\ell = 1, \ldots, N) \ , \tag{3.14}$$

The Hamiltonian in (**Eq.** (3.12) transforms to

$$H_\ell = g(a^\dagger d_\ell + a d_\ell^\dagger) \ . \tag{3.15}$$

The steady state of the system with Hamiltonian (3.15) is the vacuum for both modes a and d_ℓ where the initial state of the $(k+1)$ step is the steady state of the k step. Therefore, starting from vacuum state of the system and after performing all the N steps, the state of the N-modes becomes the

vacuum state in the space of modes $d_1, \ldots, d_N$ which is our target cluster state in the space of modes $b_1, \ldots, b_N$, i.e., $U_{C_Z}^N(A)U_{Cp}U_s|0\rangle$.

Now we show how the Hamiltonien couplings should be chosen in order to obtain the target (non Gaussian) cluster state. The unitary transformation (3.14) is proven in appendix.(B) which can be written as

$$d_\ell = \sum_{k=1}^{N} \left[U_{\ell k}\ b_k + V_{\ell k}\ b_k^\dagger + W_{\ell k} \left(b_k + b_k^\dagger \right)^2 \right] \ , \tag{3.16}$$

where the matrices U, V and W are given by the target adjacency matrix A as follows:

$$U = D_+ - \frac{i}{2}(D_+ + D_-)A \ , \tag{3.17}$$

$$V = -D_- - \frac{i}{2}(D_+ + D_-)A \ , \tag{3.18}$$

$$W = \frac{-3i}{2\sqrt{2}}\ D_\tau(D_+ + D_-) \ , \tag{3.19}$$

where the matrices $D_\pm$ and D_γ are given in terms of the squeezings r, cubicity parameters τ

$$D_+ = \mathrm{Diag}(\cosh r_1, \ldots, \cosh r_N), \tag{3.20}$$

$$D_- = \mathrm{Diag}(\sinh r_1, \ldots, \sinh r_N), \tag{3.21}$$

$$D_\gamma = \mathrm{Diag}\left(\tau_1, \ldots, \tau_N\right) \ . \tag{3.22}$$

3.3.1 Example of two-modes cluster state

In order to generate the two-mode cluster state of **Figure.** 3.7 we need two steps $\ell = 2$.

For two-mode cluster state we have $D_\pm$ and D_γ as

$$D_+ = \mathrm{Diag}(\cosh r_1, \cosh r_2), \tag{3.23}$$

$$D_- = \mathrm{Diag}(\sinh r_1, \sinh r_2), \tag{3.24}$$

$$D_\gamma = \mathrm{Diag}\left(\tau_1, \tau_2\right) \ . \tag{3.25}$$

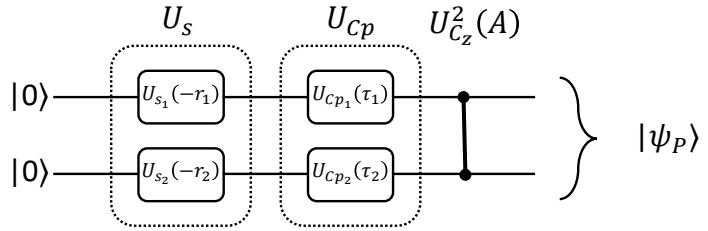


Figure 3.7: Circuit representation of two-mode approximate cluster state

and the matrices U, V and W would be

$$U = \begin{pmatrix} \cosh r_1 & -\frac{i}{2}e^{r_1} \\ -\frac{i}{2}e^{r_2} & \cosh r_2 \end{pmatrix} \tag{3.26}$$

$$V = \begin{pmatrix} -\sinh r_1 & -\frac{i}{2}e^{r_1} \\ -\frac{i}{2}e^{r_2} & -\sinh r_2 \end{pmatrix} \tag{3.27}$$

$$W = \frac{-3i}{2\sqrt{2}} \begin{pmatrix} \tau_1 e^{r_1} & 0 \\ 0 & \tau_2 e^{r_2} \end{pmatrix} \tag{3.28}$$

For the first step we have d_1 :

$$d_1 = \cosh r_1 b_1 - \sinh r_1 b_1^\dagger - \frac{i}{2}e^{r_1}(b_2 + b_2^\dagger) - \frac{3i\tau_1 e^{r_1}}{2\sqrt{2}}(b_1 + b_1^\dagger)^2. \tag{3.29}$$

we have according to **Eq.** (3.15) the Hamiltonian of the first step

$$H_1 = g(a^\dagger d_1 + a d_1^\dagger) \ . \tag{3.30}$$

For the second step d_2

$$d_2 = \cosh r_2 b_2 - \sinh r_2 b_2^\dagger - \frac{i}{2}e^{r_2}(b_1 + b_1^\dagger) - \frac{3i\tau_1 e^{r_2}}{2\sqrt{2}}(b_2 + b_2^\dagger)^2. \tag{3.31}$$

the Hamiltonian of the second step is

$$H_2 = g(a^\dagger d_2 + a d_2^\dagger). \tag{3.32}$$

The Fidelity evolution in time for this cluster state is calculated using simulation in appendix(C.2) and it is shown in **Figure.** 3.8. It is noted that the steady state we acheived of the last step is identical to the target cluster state. This proved that the switching scheme is a valid protocol our desired cluster states.

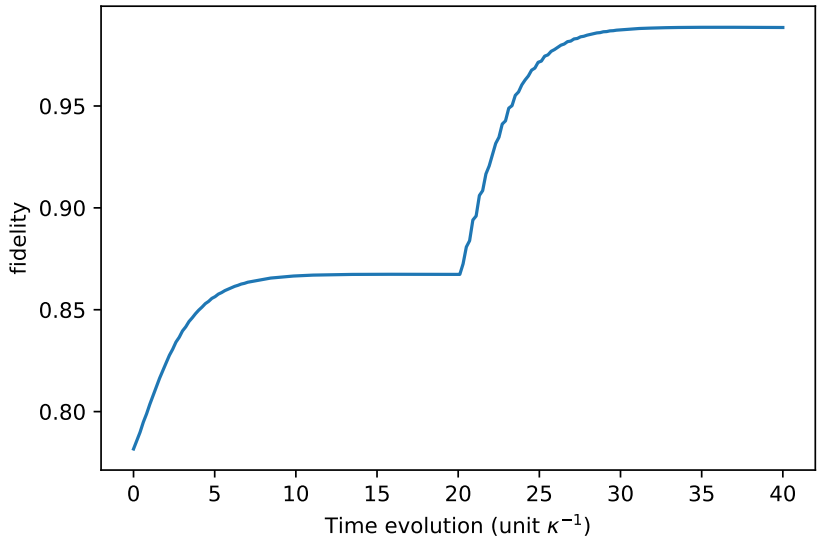


Figure 3.8: Fidelity evolution in time for two-mode cluster state with cubicity $\tau = 0.1$ and squeezing 3dB.

Conclusion

This chapter has defined the non-Gaussian cluster state and showed its ideal form and how to approximate it. After that we have given the approach [13] to generate a non-Gaussian cluster state in general form given by the switching scheme protocol and we gave an example of how to generate the two-mode non-Gaussian cluster state. Finaly we numerically proved the validity of this protocol by giving the fidelity evolution with time.

Chapter 4

Entanglement

The characterisation of quantum correlations, namely entanglement, is central to the study of quantum information. Entanglement turns out to be a key resource for the implementation of a number of quantum communication protocols, and also necessary to achieve computational speed-ups with quantum hardware, in the sense that accessing regions of the Hilbert space with entangled states allows one to shorten the computational depth of certain algorithms [28, 29]. Not surprisingly, generating and maintaining entanglement is generally difficult in practice. Thanks to the techniques developed in quantum optical set-ups to achieve squeezed light, entanglement is however relatively straightforward to produce in optical quantum continuous variables. As we shall see, in fact, continuous variable entanglement is closely related to the notion of squeezing. It is therefore of the utmost importance to be able to qualify and quantify entanglement of continuous variables, which is the subject matter of the present chapter [30].

We will present criteria to detect the entanglement of Gaussian and non-Gaussian states and then proceed to describe a possible way to quantify such quantum correlations, bearing in mind that the determination of entanglement monotones of clear operational significance is still an open problem, Especially in the restricted arena non-Gaussian states.

4.1 Entangled states and partial transposition

A bipartite quantum state ρ_{AB} is said to be separable if and only if it can be written as a mixture of product states [31]:

$$\rho_{\mathrm{AB}} = \sum_j C_j \left(\rho_{\mathrm{A},j} \otimes \rho_{\mathrm{B},j}\right), \tag{4.1}$$

where $\rho_{A,j}$ and $\rho_{B,j}$ are local quantum states of subsystems A and B, respectively. Notice that the sum could generalise to an integral over continuous, real variables. A quantum state is entangled if and only if it is not separable [31].

A general sufficient criterion to detect entanglement, and one that, as we shall see, works very well with two-mode Gaussian states, is the so called positivity of the partial transposition (PT) criterion: If ρ_{AB} is separable, and so can be written as above, the partially transposed state $\rho_{\tilde{\mathrm{A}}\mathrm{B}}$,i.e., , the state where transposition is applied to only one of the subsystems, say B, reads

$$\tilde{\rho}_{\mathrm{AB}} = \sum_j C_j \left(\rho_{\mathrm{A},j} \otimes \rho_{\mathrm{B},j}^T\right) \tag{4.2}$$

and is still a quantum state. In particular, if ρ_{AB} is separable, then $\tilde{\rho}_{\mathrm{AB}} \geq 0$ (the state is PT). Therefore, if a state is such that $\rho_{\tilde{\mathrm{A}}\mathrm{B}} \ngeq 0$, then it must be entangled (sufficient criterion for entanglement).

The PT criterion is not necessary and sufficient as there exist entangled states, termed "bound-entangled" because they cannot be distilled, which are PT [31]. Note also that the transposition basis and subsystem are irrelevant to the positivity of the partially transposed state.

4.2 Quantifying entanglement

Quantifiying entanglement is huge area of research in quantum computation where several measures of entanglement are proposed and studied according to different aim [30, 29, 32, 33, 34]. In our thesis we focus on the pure state and the best way to quantify it is using the entanglement of formation which will be discuss in this section.

Von Neumann entropy

The von Neumann entropy, named after John von Neumann, is the extension of classical Gibbs entropy concepts to the field of quantum mechanics. For a quantum-mechanical system described by a density matrix ρ, the von Neumann entropy is [30]

$$E(\rho) = -\mathrm{Tr}(\rho \ln \rho), \tag{4.3}$$

where ln denotes the (natural) logarithm.

Entanglement of formation

Entanglement of formation $E_f(\rho)$ is one of the most widely accepted entanglement measures for pure state bipartite quantum state $\rho = |\psi\rangle\langle\psi|$ where $|\psi\rangle$ is two-partite state (A and B). Entanglement of formation is defined by von Neumann entropy of reduced density matrix as [30]

$$E_f(\rho) = -\mathrm{Tr}(\rho_\mathrm{A} \ln \rho_\mathrm{A}), \tag{4.4}$$

where $\rho_\mathrm{A} = \mathrm{Tr}_\mathrm{B}\rho$ and Tr_B is the partial trace over mode B.

4.3 Wigner negativity and mana

Negativity of the Wigner function has long been recognized as an important quantum feature and in particular the volume of the negative part has been introduced as a nonclassicality quantifier [34].

In [35] a computable and additive magic monotone based on the negative values of the discrete Wigner function, dubbed *Dmana*, was introduced. We call the CV counterpart *mana*; it is defined as[1] [32]

$$\mathcal{M}(\rho) = \log\left(\int \mathrm{d}r \ |W_\rho(r)|\right), \tag{4.5}$$

where the integral runs over the whole phase-space $r \in \mathbb{R}^{2N}$, where N is the number of modes.

[1] The base of the logarithms is irrelevant for this definition and the following properties; however, in the numerical results we choose logarithms in base 2.

The maximal set of states that can be generated via Gaussian protocols (GP) namely, the Gaussian *convex* hull, is defined as

$$\mathcal{G} = \left\{ \rho \in \mathcal{H} \,|\, \rho = \int \mathrm{d}r \, p(r) \, |\psi_G(r)\rangle\langle\psi_G(r)| \right\}, \tag{4.6}$$

where $p(r)$ is an arbitrary probability distribution, $\mathcal{H}$ Hilbert space, and $|\psi_G(r)\rangle$ Gaussian state.

Once the sets of free operations and states are chosen, one can indeed try to quantify entanglement.

One can define quantum-non-Gaussianity through the mana where $\mathcal{M} \in \mathbb{R}$ which satisfies the following properties:

- $\mathcal{M}(\rho) = 0 \quad \forall \rho \in \mathcal{G}$ (resp. W_+), means that for any Gaussian states mana equal to zero
- $\mathcal{M}(\rho) \neq 0 \iff \rho \notin \mathcal{G}$ means that any states has mana differnt from zero should be non-Gaussian states

Here some Examples, suppose we have one-mode state i.e., Fock state $\rho = |1\rangle\langle 1|$, using simulation given in **Appendix** C we have the mana $\mathcal{M} = 1.0486319384594842$, notice that mana is different from zero this means only that this state is non-Gaussian state.

Now for two-mode state i.e., $\rho = \frac{1}{2}(|00\rangle + |11\rangle)(\langle 00| + \langle 11|)$, using same simulation befor we find the mana $\mathcal{M} = 12.256858847405807$, which means that this is non-Gaussian state with that quantity of mana.

4.4 Entanglement of formation and Mana for two-mode approximate cluster state

The two-mode cluster state was discussed previously in **Section** 3.3.1 where we said it is highly entangled, here we introduce how to quantify its entanglement.

4.4.1 Entanglement of formation for two-mode approximate cluster state

For two-mode cluster state ρ_{Cl_2} the evolution of entanglement of formation $E_f(\rho_{Cl_2})$ can be calculated as function of cubicity τ and squeezing s where

$s = 10 \log_{10} e^{-2r}$ dB and r squeezing parameter given in section.(1.3.2). The simulation we used to do the calculation for entanglement of formation is given in **Appendix** C.

If we fixed squeezing $s = (3, 6)$dB and we plot the evolution of $E_f(\tau)$ in cubicity $\tau \in [0.1, 1]$ we obtain the plot of the **Figure.** 4.1. And if we fixed cubicity $\tau = (0.2, 0.5)$ and we plot the evolution of $E_f(s)$ in squeezing $s \in [0, 10]$dB we will obtain plots of **Figure.** 4.2. We notice the more squeezing or cubicity, the more entanglement is contained in the cluster state. This proves that our cluster state is a highly entangled state.

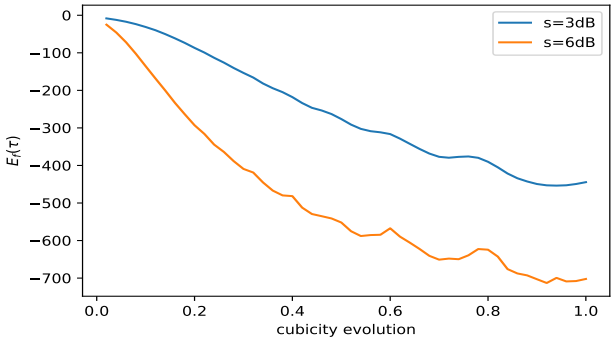


Figure 4.1: Entanglement of formation evolution in squeezing for two-mode cluster state with cubicity $\tau = (0.2, 0.5)$.

4.4.2 Wigner function of two-mode cluster state

Wigner function of one-mode cubic phase gate W_{Cp} is given in **Eq.** (1.135). The Wigner function W_{Cp_2} of a separated two-mode cubic phase states A and B (without applying U_{C_Z}) is:

$$W_{Cp_B}(x_A, p_A, x_B, p_B) = W_{Cp_A}(x_A, p_A) \times W_{Cp_B}(x_B, p_B). \tag{4.7}$$

The result of applying the controlled phase gate on the two-mode A and B is the transformation of the momentum quadratures as [13, 15]

$$\hat{p}_A \to \hat{p}_A - \hat{x}_B, \qquad \hat{p}_B \to \hat{p}_B - \hat{x}_A, \tag{4.8}$$

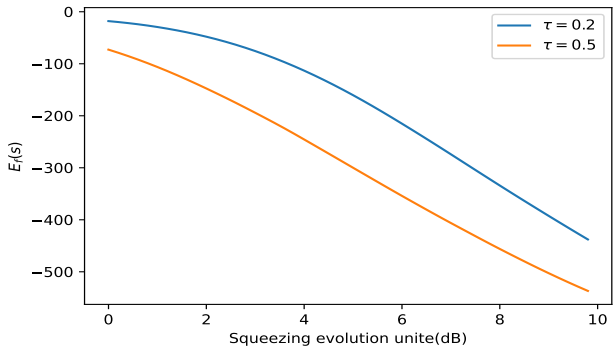


Figure 4.2: Entanglement of formation evolution in τ for two-mode cluster state with squeezing 3dB and 6dB.

The Wigner function resulting after applying U_{C_Z} is the Wigner function of two-mode cluster state and it is given as [13]

$$W_{\mathrm{Cl}_2}^{r_A,r_B,\tau_A,\tau_B}(x_A,p_A,x_B,p_B) = W_{Cp_B}(x_A,p_A-x_B,x_B,p_B-x_A) \tag{4.9}$$

$$\begin{aligned} &= \frac{2^{4/3}}{3^{2/3}\pi|\tau_A\tau_B|^{1/3}} \exp\left(\frac{1}{54}\Big(\right. \\ &\frac{e^{-6r_A}\left(1-18e^{4r_A}\tau_A(p_A-x_B)\right)}{\tau_A^2} \\ &+ \frac{18e^{-2r_B}(x_A-p_B)}{\tau_B} + \frac{e^{-6r_B}}{\tau_B^2}\Big) - r_A \\ &\left. - r_B\right)\mathrm{Ai}(Q)\mathrm{Ai}(G) \end{aligned} \tag{4.10}$$

where Ai(.) is Airy function ai.

$$\begin{aligned} Q &= \frac{2^{2/3}\left(-p_A + \frac{e^{-4r_A}}{12\tau_A} + 3\tau_A x_A^2 + x_B\right)}{\sqrt[3]{3}\sqrt[3]{|\tau_A|}}. \\ G &= \frac{2^{2/3}\left(-p_B + \frac{e^{-4r_B}}{12\tau_B} + 3\tau_B x_B^2 + x_A\right)}{\sqrt[3]{3}\sqrt[3]{|\tau_B|}}. \end{aligned}$$

4.4.3 Mana of two-mode cluster state

In order to calculate mana of two-mode cluster state ρ_{Cl_2} we substitute **Eq.** (4.9) in **Eq.** (4.5) as

$$\mathcal{M}(\rho_{\mathrm{Cl}_2}) = \log_2 \left(\int\int\int\int \mathrm{d}x_A \mathrm{d}x_B \mathrm{d}p_A \mathrm{d}p_B \left| W_{\mathrm{Cl}_2}^{\tau_A,\tau_B,\tau_A,\tau_B}(x_A, p_A, x_B, p_B) \right| \right). \tag{4.11}$$

Now, suppose we have same two-mode cluster state ρ_{Cl_2} given in **Figure.** 3.7. We choose the quadrature eigenvalues field $(x_A, x_B) \in [-5, 5]$ and $(p_A, p_B) \in [-8, 25]$ in order to integrate over the whole W_{Cl_2} field, the cubicity(τ) and the squeezing (s) given in unit (dB). Then we use simulation in appendix.(C.4) to do the integrate.

Now if we fix $\tau = (0.2, 0.5)$ and plot the mana evolution in squeezing $s \in [0, 10]$ dB we get the data of **Figure.** 4.3. And if we fixed squeezing $s = (3, 6)$ dB and we plot the mana evolution in τ where $\tau \in [0, 10]$ we get **Figure.** 4.4. Mana is increasing with both squeezing and cubicity. This is compatible with what we said before regarding the relation between entanglement with both squeezing and cubicity.

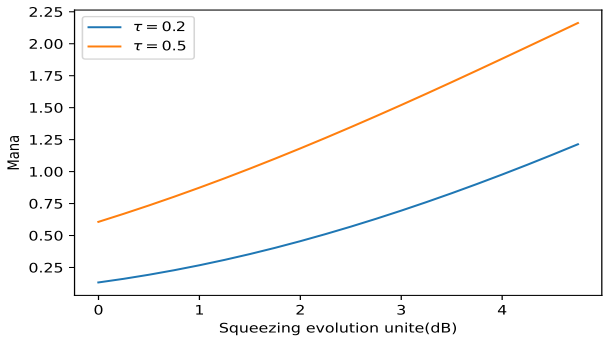


Figure 4.3: Mana evolution in squeezing for two-mode cluster state with cubicity $\tau = (0.2, 0.5)$.

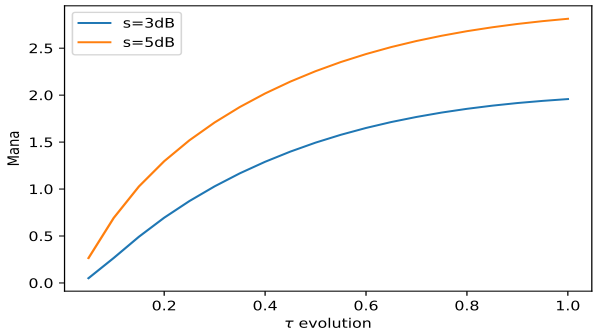


Figure 4.4: Mana evolution in τ for two-mode cluster state with squeezing 3dB and 6dB.

Conclusion

In this chapter we have given a definition for entanglement and its relation with the partial transpose. then we have seen the two main aspects of Entanglement measures. First, the entanglement of Formation which is consists of the von Neumann entropy and the partial transpose. Then we use it to quantify entanglement of two-mode cluster state and we showed how it act under evolution of squeezing and cubicity. Second, the mana or the wigner negativity which it is a perfect tool to determine the Gaussianity/Non-Gaussianity of a state or an entangled states, then we used it to quantifies entanglement of the same two-mode cluster state under evolution of squeezing and cubicity.

Chapter 5

Measurement-based quantum computation

Quantum computation (QC) is a simular process of the classical computation where instead of using classical laws we use the quantum laws. The information in classical computation is stored in bits, which takes the discrete values 0 or 1 and these bits are determined physically using classical laws (the voltage). Classical computaion is a process that simulates an input system according to a specific funtion into a different output system as in **Figure.** 5.1.

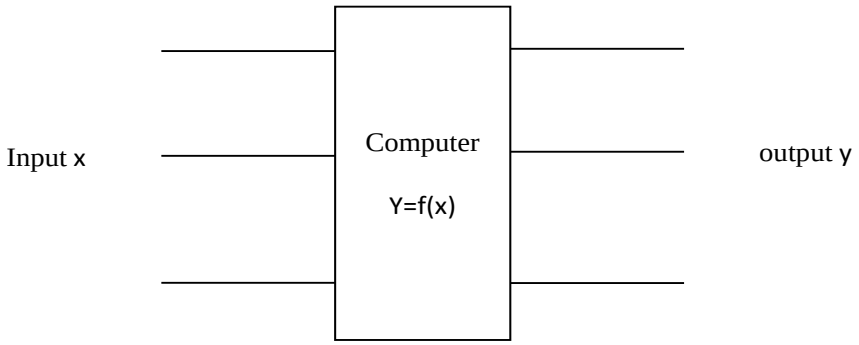


Figure 5.1: Circuit representation of a classical computer.

On the other hand, the information in QC is stored in the state of a quantum system. QC is a process that simulates the state of an input quantum

system into another state according to quantum laws, see **Figure.** 5.2 as in the following representation

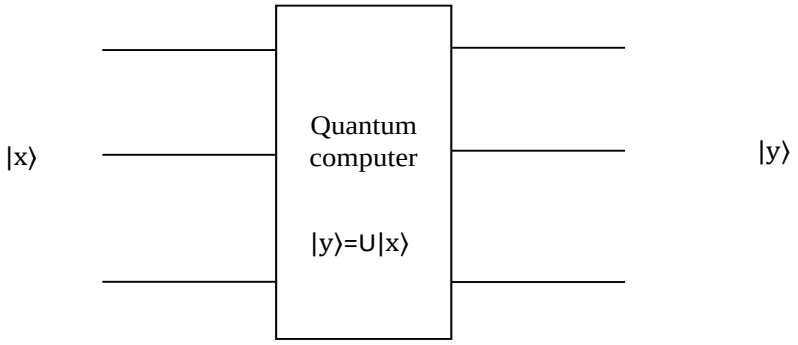


Figure 5.2: Circuit representation of a quantum computer.

Lloyd and Braunstein [23] proposed the use of CV for QC and showed that arbitrary quantum logic gates (i.e., simple unitaries) could be created using Hamiltonians that are polynomial in the quadrature operators $\hat{x}$ and $\hat{p}$ of the harmonic oscillator. and proved that only a finite set of CV gates are needed for universal QC.

5.1 Quantum computation

QIP is based on the use of the laws and properties of quantum mechanics where the information is encoded in the different states of a quantum system, and the computation is accomplished by applying a series of (unitary) transformations of these states. The result of computation (output) is obtained by appropriate measurements done on the system. The device that performs QIP is called quantum computer. [36]

The information in CV systems is encoded in an infinite-dimensional systems, and it is easier to encode information and to process it using CV systems. Here we focus on the measurement-based (one-way) model of quantum computation. [22]

5.2 Universal quantum computaion

Universal QC in the context of CV system can be reach using Gaussian and non-Gaussian measurements on Gaussian cluster state [24]. But non-Gaussian measurements are very difficult to implement [24]. To overcome this difficulty we reach the universal QC using no-Gaussian cluster state and only Gaussian measurements [13, 37, 38]. In the following we focus on using the non-Gaussian cluster state studied before as a resource for universal quantum computation.

5.2.1 Continuous-variable quantum gates

the Heisenberg-Weyl operators which comprise of the position and momentum phase-space displacement operators, given respectively as

$$X(s) = \exp(-is\hat{p}) \ , \tag{5.1}$$
$$Z(t) = \exp(it\hat{x}) \ , \tag{5.2}$$

where $X(s)$ gives a shift by an amount s in the x direction and $Z(t)$ a momentum shift by an amount t in the p direction. In terms of the displacement operator $D(\alpha)$ they can be rewritten as

$$X = D(s/2) \ , \tag{5.3}$$
$$Z = D(it/2) \ . \tag{5.4}$$

They are related via

$$X(s)Z(t) = e^{-ist/2}Z(t)X(s) \ , \tag{5.5}$$

and act on the position computational basis states $|x\rangle$ as

$$X(s)|x\rangle = |x+s\rangle \ , \tag{5.6}$$
$$Z(t)|x\rangle = e^{itx}|x\rangle \ , \tag{5.7}$$

and on the momentum basis states $|p\rangle$ as

$$X(s)|p\rangle = e^{-isp}|p\rangle \ , \tag{5.8}$$
$$Z(t)|p\rangle = |p+t\rangle \ . \tag{5.9}$$

The position and momentum basis states are related via a Fourier transform as defined in Eq.(1.32). The Fourier gate F can be defined in terms of the annihilation and creation operators as well as the quadrature operators

$$F = \exp\left[\frac{i\pi}{2}\hat{a}^\dagger\hat{a}\right] = \exp\left[\frac{i\pi}{8}\left(\hat{x}^2 + \hat{p}^2\right)\right] . \tag{5.10}$$

In the phase-space picture, the Fourier gate is a $\pi/2$ rotation,

$$F^\dagger\hat{x}F = -\hat{p} , \tag{5.11}$$
$$F^\dagger\hat{p}F = \hat{x} . \tag{5.12}$$

The Fourier gate acts on the displacement gates as follows

$$F^\dagger Z(t)F = X(t) , \tag{5.13}$$
$$FX(s)F^\dagger = Z(s) . \tag{5.14}$$

Finally, the Fourier gate acting on the quadrature eigenstates gives

$$F|Y\rangle_x = |Y\rangle_p , \tag{5.15}$$
$$F^\dagger|Y\rangle_x = -|Y\rangle_p, \tag{5.16}$$
$$F|Y\rangle_p = -|Y\rangle_x , \tag{5.17}$$
$$F^\dagger|Y\rangle_p = |Y\rangle_x, \tag{5.18}$$

5.3 Measurement-based quantum computation using continuous variables

Measurement-based QC [22] using CV [24, 25] provides the resource initially in the form of a specific entangled state known as a cluster state and performs a series of single-mode measurements on this state. This method allows us to do any computational algorithm (note that we often start our analysis using a completely entanglement state but move on to a more realistic case of a non-Gaussian mass state like the one we present).

From the postulates of quantum mechanics, we know that the measurement result is one of the eigenvalues of the measured operator, and the system state after the measurement is the eigenstate corresponding to the measured result. These two postulates are the foundation of what will come next shortly.

The two basic steps of CV cluster state quantum computation can be summarized as follows [24]:

1. Cluster state preparation: starting with the ideal version where the initial state $|\psi\rangle_p$ infinite momentum squeezed multi-mode state. The cubic phase gate applied separately in each mode. The controlled phase gate is applied to the relevant quantum modes in order to create entanglement cluster state.

2. measurement: one-mode measurements are made on the relevant quantum modes where each result is used to select the subsequent measurement basis

Suppose we have a state of a system $\phi\rangle$ represented in the Qcircuit in **Figure.** 5.3 before measuring. In order to define it we need some steps, first

$$|\psi\rangle \otimes U_{Cp}(\tau_2)|0\rangle_p = \frac{1}{\sqrt{2\pi}} \int \mathrm{d}x_1 \mathrm{d}x_2 \psi(x_1) e^{i\tau x_2^3} |x_1\rangle \otimes |x_2\rangle, \tag{5.19}$$

where $|\psi\rangle = \int \mathrm{d}x_1 \psi(x_1)|x_1\rangle$ and $U_{Cp}(\tau_2)(\tau_2)|0\rangle_p = \frac{1}{\sqrt{2\pi}} \int \mathrm{d}x_2 e^{i\tau_2 x_2^3}|x_2\rangle$. Now we apply the controlled phase gate to get the state $|\phi\rangle$

$$\begin{aligned} |\phi\rangle &= U_{C_Z}(|\psi\rangle \otimes U_{Cp}(\tau_2)|0\rangle_p), \\ &= \frac{1}{\sqrt{2\pi}} \int \int \mathrm{d}x_1 \mathrm{d}x_2 \psi(x_1) e^{i\tau x_2^3} e^{ix_1 x_2} |x_1\rangle \otimes |x_2\rangle. \end{aligned} \tag{5.20}$$

After measuring p_1 of the first mode, using the projector $|m_1\rangle\langle m_1|$, and obtaining the result m_1, the output state in the seond mode is

$$|\psi'\rangle = \frac{1}{2\pi} \int \int \mathrm{d}x_1 \mathrm{d}x_2 \psi(x_1) e^{i\tau x_2^3} e^{ix_1(x_2 - m_1)} |x_2\rangle, \tag{5.21}$$

where $\langle m_1|x_1\rangle = \sqrt{2\pi}^{-1} \exp(-ix_1 m_1)$ the state $|\psi'\rangle$ can be rewritten as

$$|\psi'\rangle = U_{Cp}(\tau_2) X(m_1) F |\psi\rangle. \tag{5.22}$$

Applying any Unitary on the first mode $U|\psi\rangle$ (see **Figure.** 5.4) gives after measuring it in the output state in the seond mode

$$|\psi'\rangle = U_{Cp}(\tau_2) X(m_1) F U |\psi\rangle. \tag{5.23}$$

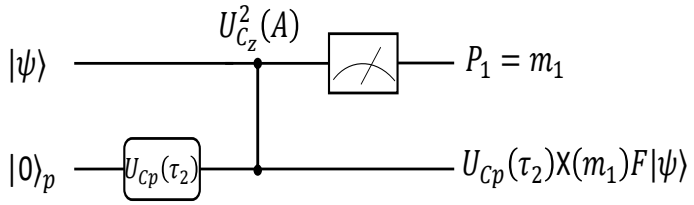


Figure 5.3: Qcircuit of measuring momentum for entangled state.

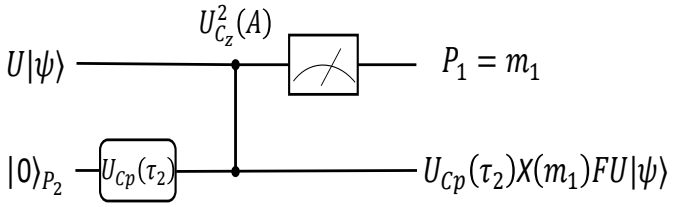


Figure 5.4: Qcircuit of measuring momentum for entangled state with applying unitary on the first mode.

So if we have an ideal cluster state like the one in figure.(5.5), After measuring p_1 of the first mode, we get on the seond mode an output state as

$$|\psi'\rangle = U_{Cp_2}(\tau_2)X(m_1)FU_{Cp_1}(\tau_1)|0\rangle_{p_1}. \tag{5.24}$$

and if we have three-mode ideal cluster state (see figure.(5.6)) and after measuring p_1 of the first mode and $p2$ of the second mode, the output state on the theard mode is

$$\begin{aligned} |\psi'\rangle \quad = \quad & \Big[\big(U_{Cp_2}(\tau_2)\,X(m_1)\,FU_{Cp_1}(\tau_1)\big) \otimes \big(U_{Cp_3}(\tau_3)\,X(m_2)\,FU_{Cp_2}(\tau_2)\big)\Big] \\ & \Big[|0\rangle_{p_1} \otimes |0\rangle_{p_2}\Big]. \end{aligned} \tag{5.25}$$

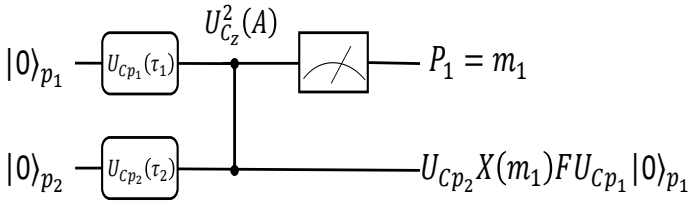


Figure 5.5: Qcircuit of measuring momentum for tow-mode ideal cluster state.

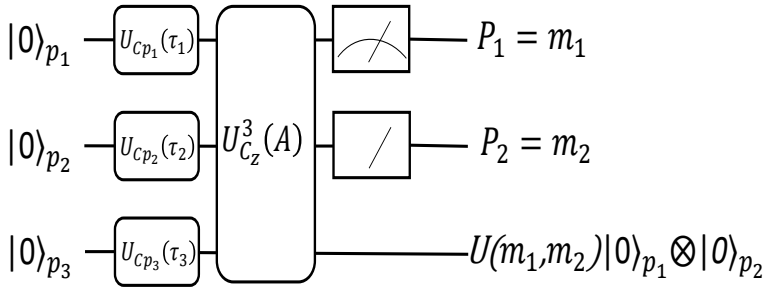


Figure 5.6: Qcircuit of measuring momentum for three-mode ideal cluster state.

5.4 Measurement-based computation of two-mode approximate cluster state using Wigner Function

Suppose we have two-mode approximate cluster state as in Qcircuit in **Figure.** 3.7. Its Wigner function W_{Cl_2} has been given in the previous chapter in **Eq.** (4.9). Now if we measured the momentum of the first mode, see **Figure.** 5.7, the output state in the second mode will be defined by the Wigner function

$$W_{\mathrm{md}_2}(x_2, p_2) = \int W_{\mathrm{Cl}_2}(x_1, m_1, x_2, p_2)\mathrm{d}x_1. \tag{5.26}$$

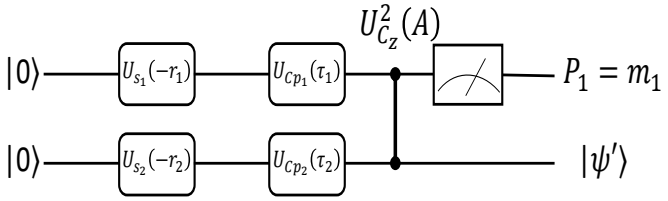


Figure 5.7: Qcircuit of measuring momentum for tow-mode ideal cluster state.

Using the integrals

$$\int_{-\infty}^{\infty} \mathrm{d}y\ e^{\lambda y}\mathrm{Ai}(ay+b) = \frac{1}{|a|}\exp\left[\frac{1}{3}\left(\frac{\lambda}{a}\right)^3 - \frac{\lambda}{a}\ b\right]\ . \tag{5.27}$$

$$\int_{-\infty}^{\infty} \mathrm{d}y\ e^{\lambda y}\mathrm{Ai}(y^2+a) = 4^{\frac{1}{3}}\pi\left|\mathrm{Ai}\left(4^{-\frac{1}{3}}(a+i\lambda)\right)\right|^2\ . \tag{5.28}$$

we have the analytic form of the Wigner Function of the output state (the average state) after measuring the first mode's momentum quadrature:

$$\begin{aligned}\int W_{\mathrm{md}_2}(x_2,p_2,m_1)\mathrm{d}m_1 \ &= \ \frac{2^{2/3}}{\sqrt[3]{3}\sqrt{\pi}\sqrt[3]{|\tau_2|}}\exp\Bigg(-\frac{p_2e^{2r_1}}{3\tau_2}+\frac{\left(e^{2r_1}+e^{-2r_2}\right)^3}{54\tau_2^2}\\ &\quad +e^{2r_1}x_2^2-r_2\Bigg)\mathrm{Ai}\Bigg(6^{2/3}x_2^2\tau_2^{2/3}-\frac{2^{2/3}p_2}{\sqrt[3]{3}\sqrt[3]{\tau_2}}\\ &\quad +\frac{\left(e^{2r_1}+e^{-2r_2}\right)^2}{6\sqrt[3]{6}\tau_2^{4/3}}\Bigg)\end{aligned} \tag{5.29}$$

Conclusion

In this thesis, we gave a review of CV quantum systems where we have introduced some of Gaussian and non-Gaussian states and their Wigner functions. These quantum states play a major role in quantum computation.

In the beginning, we started by giving a review of CV quantum systems in the phase space formalism, with introducing some of Gaussian and non-Gaussian states that play major role in generating cluster states. After that, we moved to study OQS which is a very large area of research. We gived some general definitions that we are interested in including the Markovian master equation and the steady states with some examples in order to theoretically explain how to generate quantum state.

More after, we introduced our scheme to generate an approximate non-Gaussian cluster state encoded in a set of entangled modes of an OQS. The generated non-Gaussian cluster state was obtained as a steady states on the last set of that OQS. Also, we proved that our approximate non-Gaussian cluster state is highly entangled state.

We discussed the use of the approximate non-Gaussian cluster state it as a resource of quantum computation to achieve universality. We apply a sequence of single-mode measurements on our cluster state, and we were able to define the output state, in terms of the Wigner function.

The non-Gaussian cluster state version is promising area in universal quantum computation cause it need only Gaussian measurment which is alredy wide integrated branch, many researchs were done on this topic [13, 39, 40, 41, 42]. This work opens the way to any reaserch in universal quantum computation by providing a multimode, higly entangled, non-Gaussian resource state, that with our technologies todays is very important tool to gain very accurate result, which one day help us to build a quantum computer.

Appendix A

Two-mode squeezing

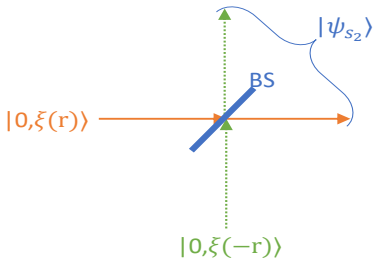


Figure A.1: A schematic diagram of the beam-splitter(BS), the input states are $|0,r\rangle_{\rm a}$ and $|0,-r\rangle_{\rm b}$ and the output state is $|\psi_{s_2}\rangle_{\rm ab}$.

These are combined via a balanced beam splitter to generate the two-mode squeezed vacuum state, where we have at first $U_{BS}|00\rangle = U_{BS}^{\dagger}|00\rangle = |00\rangle$.

$$|\psi_{s_2}\rangle_{\rm a,b} \quad = \quad U^{B}_{BS_{\rm ab}} U_{s_a} U_{s_b} U^{B\dagger}_{BS_{\rm ab}} |0\rangle_{\rm a}|0\rangle_{\rm b} \tag{A.1}$$

where U^{B}_{BS} is the Balanced beam splitter operator ($\phi = \frac{\pi}{4}$ and $\theta = 0$), $U_{s_{\rm a,b}}$ one-mode squeeze operators in $x_{\rm a}$ direction and $p_{\rm b}$ direction respectively,

with using Taylor developpement we find

$$\begin{aligned} U_{s_{\rm a}}U_{s_{\rm b}} &= \exp\left[r(a^2-a^{\dagger 2}-b^{\dagger 2}+b^2)\right] \\ &= \sum_{n=0}^{\infty}\frac{r^n}{n!}(a^2-a^{\dagger 2}-b^{\dagger 2}+b^2)^n. \end{aligned} \tag{A.2}$$

Applaying U^B_{BS} gives

$$\begin{aligned} U^B_{BS_{\rm ab}}U_{s_{\rm a}}U_{s_{\rm b}}U^{B^\dagger}_{BS_{\rm ab}} &= U^B_{BS_{\rm ab}}\left(\sum_{n=0}^{\infty}\frac{r^n}{n!}(a^2-a^{\dagger 2}-b^{\dagger 2}+b^2)^n\right)U^{B\dagger}_{BS_{\rm ab}} \\ &= =\sum_{n=0}^{\infty}\frac{r^n}{n!}U^B_{BS_{\rm ab}}\ (a^2-a^{\dagger 2}-b^{\dagger 2}+b^2)^n\ U^{B^\dagger}_{BS_{\rm ab}} \\ &= \sum_{n=0}^{\infty}\frac{r^n}{n!}\left(U^B_{BS_{\rm ab}}(a^2-a^{\dagger 2}-b^{\dagger 2}+b^2)U^{B^\dagger}_{BS_{\rm ab}}\right)^n \\ &= \exp\left[rU^B_{BS_{\rm ab}}(a^2-a^{\dagger 2}-b^{\dagger 2}+b^2)U^{B^\dagger}_{BS_{\rm ab}}\right] \end{aligned} \tag{A.3}$$

using the Hausdorff recursion formula

$$e^{\alpha A}Be^{-\alpha A} = B+\alpha[A,B]+\frac{\alpha^2}{2!}[A[A,B]]+\frac{\alpha^3}{3!}[A[A[A,B]]]+\dots\ , \tag{A.4}$$

to find the linear unitary Bogoliubov transformation of a and b given in Eq.(1.99) then we deduire

$$\begin{aligned} U^B_{BS_{\rm ab}}U_{s_{\rm a}}U_{s_{\rm b}}U^{B^\dagger}_{BS_{\rm ab}} &= \exp\left[r(ab+a^\dagger b^\dagger)\right] \\ &= U_{s_{\rm 2ab}}(r). \end{aligned} \tag{A.5}$$

where $U_{s_{\rm 2ab}}(r)$ two-mode squeeze operator in x direction. So we have

$$\begin{aligned} |\psi_{s_2}\rangle_{\rm a,b} &= U_{s_{\rm 2ab}}(\xi)|0\rangle_{\rm a}\otimes|0\rangle_{\rm b} \\ &= \sum_{n=0}^{\infty}\alpha_n|n\rangle_{\rm a}|n\rangle_{\rm b}, \end{aligned} \tag{A.6}$$

introducing $\lambda=\tanh r$, the Schmidt coefficients are given by

$$\alpha_n = \sqrt{1-\lambda^2}\sum_{n=0}^{\infty}\lambda^n. \tag{A.7}$$

Appendix B

The switching programes

In order to to find the linear unitary Bogoliubov transformation of b_ℓ

$$b_\ell \longrightarrow d_\ell = \left[U_{C_Z}^N(A)U_{Cp}U_s\right]\ b_\ell\ \left[U_{C_Z}^N(A)U_{Cp}U_s\right]^\dagger \qquad (\ell = 1,\ldots,N)\ , \tag{B.1}$$

let's start by applying the squeezing operator U_s defined in Eq.(3.11)

$$U_s b_\ell U_s^\dagger = \cosh r_\ell b_\ell - \sinh r_\ell b_\ell^\dagger. \tag{B.2}$$

Now we apply the cubicity operator U_{Cp} defined in Eq.(3.2) on Eq.(B.2)

$$U_{Cp}U_s b_\ell U_s^\dagger U_{Cp}^\dagger = \cosh r_\ell b_\ell - \sinh r_\ell b_\ell^\dagger - \frac{3i\tau_\ell e^{r_\ell}}{2\sqrt{2}}(b_\ell + b_\ell^\dagger)^2. \tag{B.3}$$

Then finally we apply the controlled phase operator $U_{C_Z}(A)$ defined in Eq.(3.4) on Eq.(B.3)

$$d_\ell = \cosh r_\ell + \sinh r_\ell - i \sum_{l,k=1;\ k>l}^{N} g_{lk} e^{r_\ell}(b_k + b_k^\dagger) - \frac{3i\tau_\ell e^{r_\ell}}{2\sqrt{2}}(b_\ell + b_\ell^\dagger)^2. \tag{B.4}$$

Then we write d_ℓ in matricial form given in Eq.(3.16)

Appendix C

Simulation codes

Numerical simulations given in this thesis were produced by a set of Mathematica programs and Python(Qutip) scripts. Mathematica was used to calculate covraiance matrices, the wigner funtions and to produce it's plots, while Python was used to calculate quantum fidelities, entanglement of formation and mana and produce their plot's. in the following we give the most important section of Python script that generate different type of simulations

C.1 Fidelity of examples

```
# load packages
from qutip import *
import numpy as np
import matplotlib.pyplot as plt

# system parameters
d1=5
d2=15
d3=15
kappa=1.0
g=10*kappa
n_th1=0.0
n_th2=0.1
n_th3=0.2
theta=0             #squeezing direction
tau=0.1             # cubicity
s=3.0               # squeezing parameter s(r)
r=s*np.log(10.)/20.
```

```
mu=np.cosh(r)
nu=np.exp(1j*2*theta)*np.sinh(r)
z=r*np.exp(1j*2*theta)

# simulation parameters
T=20/kappa      # evolution time
N=100           # time data points

# field operators sys 1 and sys 2
a=tensor(destroy(d1),identity(d2))           # annihilation
    mode 1 state(1,2)
b=tensor(identity(d1),destroy(d2))           # annihilation
    mode 2 state(1,2)
s1=squeeze(d1,z)
s2=squeezing(a,b,z)

# Hamiltonian of one-mode squeezed state(1)
H=g*(a*(mu*b.dag()+nu*b)+a.dag()*(mu*b+np.conj(nu)*b.dag()))

# Hamiltonian of cubic phase state(2)
H1=g*(a*(mu*b.dag()+nu*b)+a.dag()*(mu*b+nu*b.dag())+((3*1j*
    tau)/(2*np.sqrt(2)))*(mu-nu)*(a-a.dag())*(b**2+b*b.dag()+b
    .dag()*b+(b.dag())**2))                          #
    Hamiltonian

# field operators sys 3
a=tensor(destroy(d1),identity(d2),identity(d3))
      # annihilation mode 1 state 3
b_1=tensor(identity(d1),destroy(d2),identity(d3))
      # annihilation mode 2 state 3
b_2=tensor(identity(d1),identity(d2),destroy(d3))
      # annihilation mode 3 state 3
x=position(d2)                                       # d is
    the dimension for the Hilbert space
cubic_gate=(1j*tau*x**3).expm()*squeeze(d2,z1)       # cubic
    phase gate unitary: xi=squeezing parameter
cubic_state=cubic_gate*basis(d2,0)

# Hamiltonian of two-mode squeezed state(3)
mu=np.cosh(r)
nu=-np.sinh(r)
z1=-r
H2=g*(a.dag()*(mu*b_1+np.conj(nu)*b_2.dag())+a*(nu*b_2+mu*b_1
    .dag()))+w*(mu*nu*(b_1**2+b_2**2)+mu*np.conj(nu)*(b_1.dag
    ()**2+b_2.dag()**2)+(mu**2+abs(nu)**2)*(b_1*b_2.dag()+b_1.
```

```
    dag()*b_2))

rho0=tensor(thermal_dm(d1,n_th1),thermal_dm(d2,n_th2)

# dissipation operator list
c_op=[np.sqrt(kappa)*a]

# time array
t=np.linspace(0,T,N)

# target state
rho_target=tensor(basis(d1,0),s1*basis(d2,0))
          # target state 1
rho_target=tensor(basis(d1,0),cubic_state)
          # target state 2
rho_target=tensor(basis(d1,0),s*tensor(basis(d2,0),basis(d3
    ,0)))    # target state 3
# Part 1: the dynamics
    # solving the master equation
rho=mesolve(H,rho0,t,c_op)              # state 1
rho1=mesolve(H1,rho0,c_op)              # state 2
rho2=mesolve(H2,rho2,c_op)              # state 3
    # calculating the fidelities
# fidelity sys 1
fid=np.zeros(N)
for j in range(N):
    fid[j]=fidelity(rho.states[j],rho_target)
# fidelity sys 2
fid1=np.zeros(N)
for j in range(N):
    fid1[j]=fidelity(rho1.states[j],rho_target)
# fidelity sys 3
fid2=np.zeros(N)
for j in range(N):
    fid2[j]=fidelity(rho2.states[j],rho_target)
```

C.2 Fidelity of two-mode cluster state

```
# load packages
from qutip import *
import numpy as np
import matplotlib.pyplot as plt

# system parameters
d1=5
```

```
d2=16
d3=16
kappa=1.0
g=7*kappa
n_th1=0.1
n_th2=0.0
n_th3=0.0

tau_1=0.1
tau_2=0.1

s_1=2.0              # squeezing
s_2=2.0
r_1=dB_1*np.log(10.)/20.
r_2=dB_2*np.log(10.)/20.
z_1=-r_1
z_2=-r_2

# simulation parameters
T_1=40/kappa      # evolution time step1
T_2=20/kappa      # evolution time step2
N=10              # time data points


# field operators
a=tensor(destroy(d1),identity(d2),identity(d3))
       # annihilation mode 1
b_1=tensor(identity(d1),destroy(d2),identity(d3))
       # annihilation mode 2
b_2=tensor(identity(d1),identity(d2),destroy(d3))
       # annihilation mode 3

s_1=tensor(squeeze(d2,z_1),identity(d3))
       # squeezing operator mode 1
s_2=tensor(identity(d2),squeeze(d3,z_2))
       # squeezing operator mode 2

x_1=tensor(position(d2),identity(d3))
x_2=tensor(identity(d2),position(d3))

cubic_gate_1=(1j*tau_1*(x_1)**3).expm()                    #
    cubic phase gate unitary mode 1
cubic_gate_2=(1j*tau_2*(x_2)**3).expm()                    #
    cubic phase gate unitary mode 1
cphasez=(1j*(x_1)*(x_2)).expm()                            #
```

```
    controlled phase gate untary
46
47 # Hamiltonian of step 1 and step 2
48 H_1=g*(np.cosh(r_1)*a.dag()*b_1-np.sinh(r_1)*a.dag()*b_1.dag
   ()-(1j/2)*np.exp(r_1)*a.dag()*(b_2+b_2.dag())-((3*1j*tau_1
   *np.exp(r_1)/(2*np.sqrt(2))))*a.dag()*(b_1+b_1.dag())**2+
   np.cosh(r_1)*a*b_1.dag()-np.sinh(r_1)*a*b_1+(1j/2)*np.exp(
   r_1)*a*(b_2+b_2.dag())+((3*1j*tau_1*np.exp(r_1))/(2*np.
   sqrt(2)))*a*(b_1+b_1.dag())**2)                          #
    Hamiltonian step1
49 H_2=g*(np.cosh(r_2)*a.dag()*b_2-np.sinh(r_2)*a.dag()*b_2.dag
   ()-(1j/2)*np.exp(r_2)*a.dag()*(b_1+b_1.dag())-((3*1j*tau_2
   *np.exp(r_2)/(2*np.sqrt(2))))*a.dag()*(b_2+b_2.dag())**2+
   np.cosh(r_2)*a*b_2.dag()-np.sinh(r_2)*a*b_2+(1j/2)*np.exp(
   r_2)*a*(b_1+b_1.dag())+((3*1j*tau_2*np.exp(r_2))/(2*np.
   sqrt(2)))*a*(b_2+b_2.dag())**2)                          #
    Hamiltonian step2
50
51 rho0=tensor(thermal_dm(d1,n_th1),thermal_dm(d2,0),thermal_dm(
   d3,0))     # initial state
52
53 # dissipation operator list
54 c_op=[np.sqrt(kappa)*a]
55
56 # time array
57 t=np.linspace(0,T_2,N)
58
59 # target state
60 cluster_state=cphasez*cubic_gate_1*s_1*cubic_gate_2*s_2*
   tensor(basis(d2,0),basis(d3,0))
61 rho_target=tensor(basis(d1,0),cluster_state)
62
63 # Part 1: the dynamics
64    # solving the master equation
65 rho_1=mesolve(H_1,rho0,t,c_op)              # step 1
66 for i in range(N):
67       rho_1ss=rho_1.states[N-1]
68 rho_2=mesolve(H_2,rho_1ss,t,c_op)           # step 2
69
70   # calculating the fidelities
71 fid=np.zeros(2*N)
72 for j in range(N):
73     fid[j]=fidelity(rho_1.states[j],rho_target)
74 for i in range(N,2*N):
75     fid[i]=fidelity(rho_2.states[i-N],rho_target)
```

C.3 Entanglement of formation for tow-mode cluster state

```
from qutip import *
import numpy as np
import matplotlib.pyplot as plt
from numpy import linalg as LA
import scipy as sp

    # system parameters
d1=30
d2=30
    # cubicity parameter

N=50
tau=np.zeros(N)
for i in range(1,N+1,1):
    tau[i-1]=i/50
    # squeezing parameter
dB_1=3.0
dB_2=3.0
r1=dB_1*np.log(10.)/20.
r2=dB_2*np.log(10.)/20.
z_1=-r1
z_2=-r2
    # defining entanglement of formation for two-mode cluster
    state
def Ecubic(i,j,d1,d2,z_1,z_2,tau1,tau2):
    # field operators
        # squeezing operators:
    s_1=tensor(squeeze(d1,z_1),identity(d2))
         #d1 is the dimension for the Hilbert space of mode 2
    s_2=tensor(identity(d1),squeeze(d2,z_2))
         #d2 is the dimension for the Hilbert space of mode 2

    x1=tensor(position(d1),identity(d2))
    x2=tensor(identity(d1),position(d2))
        # cubic phase gate unitarys:
    cubic_gate_1=(1j*tau1*(x1)**3).expm()
    cubic_gate_2=(1j*tau2*(x2)**3).expm()
        # ccontrolled phase gate unitary:
    cphasez=(1j*x1*x2).expm()
        #cluster state:
    ket=cphasez*cubic_gate_1*cubic_gate_2*s_1*s_2*tensor(
```

```
   basis(d1,0),basis(d2,0))
    rho=ket2dm(ket)
    rhoa=partial_transpose(rho,[i,j])
    return np.real(-1*(rhoa*np.log(rhoa)).trace())

    #calculating entanglement of formation
E1=Ecubic(0,1,d1,d2,z_1,z_2,tau1,tau2)
```

C.4 Mana of two-mode cluster state

```
from qutip import *
import numpy as np
import mpmath as mp
import scipy as sp
import matplotlib.pyplot as plt

    # cubicity parameter
N=30
tau1=0.2
tau2=0.2

    # squeezing parameter
dB_1=20.0
dB_2=20.0
r1=dB_1*np.log(10.)/20.
r2=dB_2*np.log(10.)/20.

    # simulation parameters
# integral limits
x1min=-8
x1max=8
x2min=-8
x2max=8

p1min=-5
p1max=25
p2min=-5
p2max=25

# integral piont
Nx1=80
Nx2=80
Np1=80
Np2=80

```

```
    # defining functions
def Ai(x):       # ai airy function
    ai,aip,bi,bip=sp.special.airy(x)
    return ai

def wigner2(x1,p1,x2,p2,r1,r2,Gamma1,Gamma2):
    ai1=(2**(2/3)*(-p1+x2+np.exp(-4*r1)/(12*tau1)+3*(x1)**2*
    tau1))/(3**(1/3)*abs(tau1)**(1/3))
    ai2=(2**(2/3)*(-p2+x1+np.exp(-4*r2)/(12*tau2)+3*(x2)**2*
    tau2))/(3**(1/3)*abs(tau2)**(1/3))
    wig2=(2*2**(1/3)*np.exp(-r1-r2+(1/54)*((np.exp(-6*r1)
    *(1-18*np.exp(4*r1)*(p1-x2)*tau1))/tau1**2+np.exp(-6*r2)/
    tau2**2+(18*np.exp(-2*r2)*(-p2+x1))/tau2))*Ai(ai1)*Ai(ai2)
    )/(3**(2/3)*np.pi*abs(tau1*tau2)**(1/3))
    return np.real(wig2)

def mana2(x1min,x1max,Nx1,p1min,p1max,Np1,x2min,x2max,Nx2,
    p2min,p2max,Np2,r1,r2,tau1,tau2):     # mana function

  # prepare the arrays
    x1=np.linspace(x1min,x1max,Nx1)
    p1=np.linspace(p1min,p1max,Np1)
    x2=np.linspace(x2min,x2max,Nx2)
    p2=np.linspace(p2min,p2max,Np2)

    X1,P1,X2,P2=np.meshgrid(x1,p1,x2,p2)

    I=np.zeros((Np1,Nx2,Np2))
    J= np.zeros((Nx2,Np2))
    K= np.zeros(Np2)

  # evaluate the |wigner| function at every point
    wig2=abs(wigner2(X1,P1,X2,P2,r1,r2,tau1,tau1))

  # integrate |wigner| function over all space
    for i in range(Nx1):
        I[i] = sp.integrate.simps(wig2[i,:],x1)
    for i in range(Np1):
        J[i] = sp.integrate.simps(I[i,:],p1)
    for i in range(Nx2):
        K[i] = sp.integrate.simps(J[i,:],x2)
    M = sp.integrate.simps(K,p2)

  # return result
    print(M)
```

```
75      return np.log(M)/np.log(2.0)
76
77      # calculate mana
78  mana=mana2(x1min,x1max,Nx1,p1min,p1max,Np1,x2min,x2max,Nx2,
        p2min,p2max,Np2,r1,r2,tau1,tau2)
```

Bibliography

[1] Houhou, O.: Continuous variable cluster states in optomechanical systems. PhD thesis, University of Constantine 1, Constantine (2016)

[2] Weedbrook, C., Pirandola, S., García-Patrón, R., Cerf, N.J., Ralph, T.C., Shapiro, J.H., Lloyd, S.: Gaussian quantum information. Rev. Mod. Phys. **84** (May 2012) 621–669

[3] Ferraro, A., Olivares, S., Paris, M.G.: Gaussian states in continuous variable quantum information. arXiv preprint quant-ph/0503237 (2005)

[4] Wigner, E.: Phys rev 40: 749; see also hillery. M., O'Connell, RF, Scully, MO, Wigner, EP (1984) Phys Rep **106** (1932) 121

[5] Serafini, A.: Continuous variables quantum information. (2020)

[6] Morin, O.: Non-Gaussian states and measurements for quantum information. Theses, Université Pierre et Marie Curie - Paris VI (December 2013)

[7] Lvovsky, A.I.: Squeezed light. Photonics: Scientific Foundations, Technology and Applications **1** (2015) 121–163

[8] Dybwad, J.P.: Refractively scanned interferometer (March 31 1987) US Patent 4,654,530.

[9] Unruh, W.: Quantum non-demolition. In: Gravitational Radiation, Collapsed Objects and Exact Solutions. Springer (1980) 385–426

[10] Braginsky, V.B., Khalili, F.Y.: Quantum nondemolition measurements: the route from toys to tools. Reviews of Modern Physics **68**(1) (1996) 1

[11] Schrödinger, E.: Die gegenwärtige situation in der quantenmechanik. Naturwissenschaften **23**(49) (1935) 823–828

[12] Gerry, C., Knight, P.: Quantum superpositions and schrödinger cat states in quantum optics. American Journal of Physics **65**(10) (1997) 964–974

[13] Houhou, O., Moore, D.W., Sougato, B., Ferraro, A.: Unconditional measurement-based quantum computation with optomechanical continuous variables. arXiv preprint arXiv:1809.09733 (2018)

[14] Gottesman, D., Kitaev, A., Preskill, J.: Encoding a qubit in an oscillator. Physical Review A **64**(1) (2001) 012310

[15] Brunelli, M., Houhou, O.: Linear and quadratic reservoir engineering of non-gaussian states. Physical Review A **100**(1) (2019) 013831

[16] Rivas, Á., Huelga, S.F.: Introduction to the time evolution of open quantum systems. Technical report (2011)

[17] Gardiner, C., Zoller, P., Zoller, P.: Quantum noise: a handbook of Markovian and non-Markovian quantum stochastic methods with applications to quantum optics. Springer Science & Business Media (2004)

[18] Davies, E.B.: Quantum theory of open systems. Academic Press (1976)

[19] Nielsen, M.A., Chuang, I.L.: Quantum computation and quantum information. (2000)

[20] Uhlmann, A.: The "transition probability" in the state space of a* algebra. Reports on Mathematical Physics **9**(2) (1976) 273–279

[21] Jozsa, R.: Fidelity for mixed quantum states. Journal of modern optics **41**(12) (1994) 2315–2323

[22] Raussendorf, R., Briegel, H.J.: A one-way quantum computer. Physical Review Letters **86**(22) (2001) 5188

[23] Lloyd, S., Braunstein, S.L.: Quantum computation over continuous variables. In: Quantum information with continuous variables. Springer (1999) 9–17

[24] Menicucci, N.C., Van Loock, P., Gu, M., Weedbrook, C., Ralph, T.C., Nielsen, M.A.: Universal quantum computation with continuous-variable cluster states. Physical review letters **97**(11) (2006) 110501

[25] Zhang, J., Braunstein, S.L.: Continuous-variable gaussian analog of cluster states. Physical Review A **73**(3) (2006) 032318

[26] Houhou, O., Aissaoui, H., Ferraro, A.: Generation of cluster states in optomechanical quantum systems. Physical Review A **92**(6) (2015) 063843

[27] Carmichael, H.: An open system approach to quantum optics, vol. m 18 of lecture notes in physics (1993)

[28] Vidal, G., Werner, R.F.: Computable measure of entanglement. Physical Review A **65**(3) (2002) 032314

[29] Vidal, G.: Entanglement monotones. Journal of Modern Optics **47**(2-3) (2000) 355–376

[30] Fan, H., Matsumoto, K., Imai, H.: Quantify entanglement by concurrence hierarchy. Journal of Physics A: Mathematical and General **36**(14) (2003) 4151

[31] Wolf, M.: Partial Transposition in Quantum Information Theory. (2003)

[32] Albarelli, F., Genoni, M.G., Paris, M.G., Ferraro, A.: Resource theory of quantum non-gaussianity and wigner negativity. Physical Review A **98**(5) (2018) 052350

[33] Ahmadi, M., Dang, H.B., Gour, G., Sanders, B.C.: Quantification and manipulation of magic states. Physical Review A **97**(6) (2018) 062332

[34] Kenfack, A., Życzkowski, K.: Negativity of the wigner function as an indicator of non-classicality. Journal of Optics B: Quantum and Semiclassical Optics **6**(10) (2004) 396

[35] Veitch, V., Mousavian, S.H., Gottesman, D., Emerson, J.: The resource theory of stabilizer quantum computation. New Journal of Physics **16**(1) (2014) 013009

[36] Imamog, A., Awschalom, D.D., Burkard, G., DiVincenzo, D.P., Loss, D., Sherwin, M., Small, A., et al.: Quantum information processing using quantum dot spins and cavity qed. Physical review letters **83**(20) (1999) 4204

[37] Yuen, H.P., Chan, V.W.: Noise in homodyne and heterodyne detection. Optics letters **8**(3) (1983) 177–179

[38] Collett, M., Loudon, R., Gardiner, C.: Quantum theory of optical homodyne and heterodyne detection. Journal of Modern Optics **34**(6-7) (1987) 881–902

[39] Yukawa, M., Ukai, R., Van Loock, P., Furusawa, A.: Experimental generation of four-mode continuous-variable cluster states. Physical Review A **78**(1) (2008) 012301

[40] Ra, Y.S., Dufour, A., Walschaers, M., Jacquard, C., Michel, T., Fabre, C., Treps, N.: Non-gaussian quantum states of a multimode light field. Nature Physics **16**(2) (2020) 144–147

[41] Walshe, B.W., Mensen, L.J., Baragiola, B.Q., Menicucci, N.C.: Robust fault tolerance for continuous-variable cluster states with excess antisqueezing. Physical Review A **100**(1) (2019) 010301

[42] Menicucci, N.C.: Fault-tolerant measurement-based quantum computing with continuous-variable cluster states. Physical review letters **112**(12) (2014) 120504